The Design of a Magnetic Component for Induction Brazing

Benjamin Pearce

Supervised by:
Dr Craig Baguley

A Thesis submitted to Auckland University of Technology in fulfilment of the requirements for the degree of Master of Engineering.

2019

School of Engineering and Mathematical Sciences

Abstract

Within the mining industry, jaws are used for drilling in large quantities. Slots are milled in each jaw, into which tungsten-carbide teeth are fitted and brazed. The current brazing process requires heating the whole jaw in a furnace for 4 hours, an inefficient and time consuming process. Induction brazing offers a much faster, cheaper alternative that reduces electricity consumption. Through the development of a concentrated induction coil, consistent uniform brazing can be achieved.

For brazing at high production rates a furnace- based technique has disadvantages. These include inconsistency in outcomes, low efficiency and high electricity demand. Induction brazing offers improvements in these respects, particularly if magnetic fields can be focused to give selective heating. However, difficulties may be experienced when brazing metals of dissimilar size and magnetic properties, as magnetic field penetration may be insufficient to give rapid heating of the brazing filler metal. This research proposes a coil design that guides the magnetic field to give penetration at desired locations, despite the presence of materials that could otherwise act as a magnetic shield. Magnetic modelling using the finite element method is presented, considering variations in magnetic diffusivity and skin depth in the approach to Curie temperatures. Comparison to a coil without magnetic field guidance indicates the proposed coil achieves superior performance.

This study will add to the scientific knowledge in the field of induction heating, specifically in the area of ensuring that a magnetic field penetrates to a brazing region surrounded on all sides by conductive materials with differing properties.

To

Lydia, Mum and Dad

Acknowledgements

Firstly I would like to express my deepest gratitude to my supervisor Dr Craig Baguley, who inspired me to carry out this research project and continuously supported and guided me throughout the duration of my studies. He has generously and patiently shared his time, knowledge and expertise with me, for which I am most thankful for. I have learnt a tremendous amount being under his supervision and without his input this research would not have been possible.

I also extend my thanks to the staff at Heat Treatments, in particular Fergus Thompson and Keith McGregor for providing me with the opportunity to work with their company in the practical implementation of this research.

I also would like to thank Callaghan Innovation for the research and development grant which I am most grateful to have received.

I would like to thank my parents, David and Claire Pearce, who have encouraged, supported and provided for me throughout the years of my study and the duration of my masters. I am beyond grateful to have been blessed with such loving and thoughtful parents.

Finally I would like to express my gratitude to my beautiful wife, Lydia, who has been of great support to me during these final months of this research work. I want to thank her for her understanding and appreciation of the work involved in such research work, and for encouraging me through the difficult times.

Table of Contents

Attestation of Authorship

I hereby declare that this submission is my own work and that, to the best of my knowledge and belief, it contains no material previously published or written by another person (except where explicitly defined in the acknowledgements), nor material which to a substantial extent has been submitted for the award of any other degree or diploma of a university or other institution of higher learning.

Signed:

08/03/2019

Confidential Material

All images, dimensions, and descriptions of the jaws produced by Heat Treatments Ltd are confidential and **must not** be published on the internet or any database unless approval has been given by the Author and Heat Treatments Ltd. Confidential content is throughout the Thesis and, therefore, a PGR16 has been submitted with this Thesis.

List of Figures

List of Tables

Nomenclature

Acronyms

EMF	electro motive force
FEM	finite element method
MDM	magneto-dielectric materials
MMF	magneto-motive force
IPT	inductive power transfer

Symbols

Small Characters

c	specific heat of material
e	emissivity of work surface
h	induced heat
l	length of path through material
l_{gap}	length of path through gap
$l_{material}$	length of path through material
m	mass
r	distance between coil and work piece

Capital Letters

A	surface area
A_g	cross sectional area air gap
$A_{material}$	cross sectional area material
$A_{\perp}^{macro}$	surface area
B	magnetic flux density
E(k)	complete elliptic integral function second kind
G	air gap area
H_0	magnetic field strength

I	induced current
I_c	coil current
$I_{macro}(t)$	induced eddy currents
K(k)	complete elliptic integral function first kind
M1	flux concentrator area
P_1	load power
P_2	radiation losses
P_3	power loss in induction coil
P_f	face permeance
P_{hb}	horizontal bypass permeance
P_{hl}	horizontal leakage permeance
P_{macro}	induced power
$\bar{P}_R$	mean heating power
P_T	total power
P_{vb}	vertical bypass permeance
P_{vl}	vertical slot leakage permeance
R	electrical resistance of conductor
R_c	AC coil resistance
Sn-Pb	Tin-lead
T_1	work piece temperature
T_2	ambient temperature
T_X	transmitting coil

Greek Letters

δ	skin depth
ΔT	change in temperature
$\varepsilon(t)$	electro motive force
η_H	overall heating efficiency
κ_0	magnetic diffusivity
μ	permeability
μ_o	$4\pi \times 10^{-7}$
μ_r	relative permeability

σ	electrical conductivity
ϕ	flux
ω	frequency

Chapter 1

Introduction

1.1 Research Background

Within the mining industry in Australia, jaws are used in very large numbers to grip drilling shafts. Each jaw comprises a 1020 mild steel bulk, into which slots are milled and tungsten-carbide inserts are placed, as shown in Fig. 1(a). The tungsten-carbide inserts improve grip and wear properties and are attached to the 1020 mild steel through brazing. A New Zealand based company, Heat Treatments Ltd [1], currently uses the vacuum furnace shown in Fig. 1 (b) to braze these jaws. The current brazing process involves four steps. Initially a worker cleans each of the 1020 mild steel bulks to remove any oils or contaminants. The worker then applies flux and alloy to the slots, before placing the tungsten-carbide inserts. Next, the jaws are loaded into an electric vacuum furnace on a 4 hour cycle. Once treating is complete the jaws are removed and allowed to cool, before being bead blasted and inspected. This production process is slow, labour intensive and demands high levels of energy. To add to this, approximately 5% of jaws need re-working, as the inserts have not seated, or brazed properly. These require correction by a skilled worker.

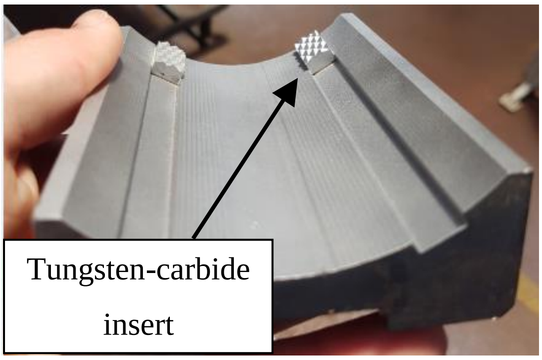

(a)

(b)

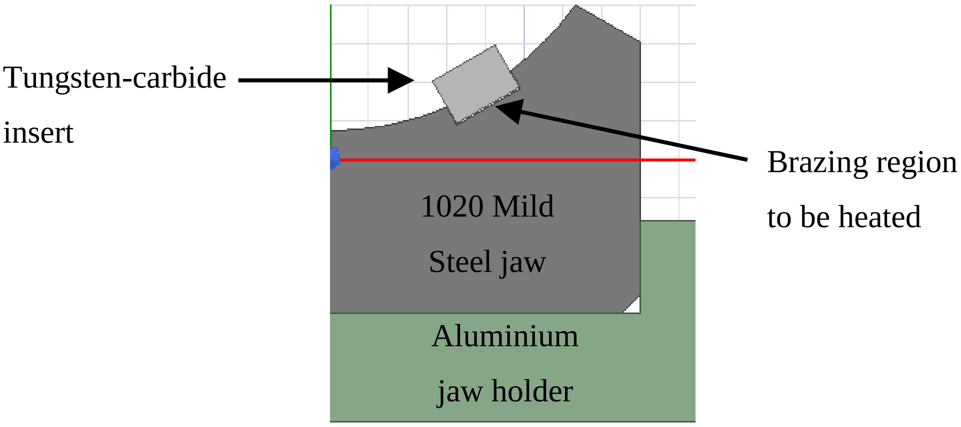

(c)

Fig. 1 – (a) Slotted 1020 mild steel work-piece with tungsten-carbide insert fitted, (b) Heat Treatments vacuum furnace, (c) Cross sectional view of right hand side of jaw

A potentially faster, cheaper and more energy efficient production process is to induction braze. In this case the jaw assembly can simply be placed under an energised induction coil, which generates a magnetic field that induces eddy currents, losses and heat in the work-piece. If correctly designed, this process can reduce heating time from hours to seconds. Further, an induction brazing step can be easily integrated into an automated manufacturing process [2]. However, significant challenges exist for the specific induction brazing process Heat Treatments requires. These include the difficulty of transferring heat into the region where brazing takes place, as this region is shielded on all sides. This can be observed in Fig. 1 (c). A reported approach that overcomes this difficulty involves heating the entire body of a work-piece, including the brazing region [3]. However, this is very energy inefficient. In this Thesis an improved approach is proposed, which uses a focussed magnetic field to concentrate heat at the brazing region without incurring significant and undesired losses in other regions. Further, the proposed solution overcomes difficulties associated with differences in the magnetic and thermal properties of the tungsten-carbide and 1020 mild steel materials surrounding the brazing region. This was achieved through undertaking research on modelling using the finite element method (FEM), and allowing for skin effect and relative changes in tungsten-carbide and 1020 mild steel material properties with temperature. The results of the modelling were used to develop a solution that was implemented. The implemented result was successful, and the experimental results verify the modelling effort. According to literature, such a solution has not been previously reported. Therefore, and on this basis, the work presented in this Thesis is a scientific contribution to knowledge on induction brazing.

While the experimental work successfully demonstrated improved induction brazing performance, this proposed solution is not optimal, as the frequency of the applied magnetic field was constrained by limitations of the magnetic field generator. Ideally, and according to research shown in this Thesis, a lower operating frequency would be superior. Further, and with the use of a magnetic field concentrator implemented using a magnetic material that can be shaped as desired, further gains are possible. This claim is supported through the results of FEM modelling that are also presented in this Thesis.

1.2 Research Questions

To achieve true localised heating, eddy currents need to be focussed in the brazing region of the work-piece required to be heated. For this to be achieved there are several variables that must be considered. The first of which is the shape of the magnetic field produced by the work-coil, as eddy currents will be induced where lines of magnetic flux intercept the work-piece. If this field is not concentrated effectively, the result will be slower heating and increased power consumption. The second variable relates to the depth at which eddy currents penetrate the jaw, which affects the speed of heating and the power consumption. Thus, the operating frequency of the power supply should be such that balance is achieved between power draw and heating time.

The questions to be addressed in this thesis therefore are:

1. What is the optimal coil design to induction braze a work-piece, subject to a number of constraints.

   These include:

   - Localizing the applied magnetic field, in so far as possible, to the area in need of heating and ensuring uniformity of heating over the brazing region
   - Ensuring the magnetic field strength is great enough to rapidly heat the work-piece, before the heat is drawn away through conduction (slow heating will prevent high, local temperatures being attained and result in mild steel scaling)
   - Compliance to a design constraint that limits how closely the induction coil can be placed to the work-piece

2. What is the optimal frequency to achieve minimal power consumption whilst maintaining effective localised heating between dissimilar metals?

   This presents a significant challenge, as the brazing region is surrounded on all sides. Given the differing magnetic and thermal properties of the tungsten-carbide inserts and 1020 mild steel, shielding of the brazing region may result if the operational frequency is too high and, therefore, incur reliance on thermal conduction. This is inefficient. Similarly, if the frequency is too low, increased power draw and heating time will result, as the skin depth will be greater and losses will be induced in larger region than desired.

1.3 Thesis Structure

The chapters of this Thesis are arranged as follows:

In Chapter 2 a systematic review of previous investigations in the fields of induction brazing and electromagnetic field concentration is presented. This identifies a knowledge gap surrounding the design of efficient induction process for brazing applications in which the region to be brazed is shielded on all sides. Methods of electromagnetic field concentration and field analyses are also reviewed and evaluated.

In Chapter 3 previous work and a commercial solution to the application is presented and critically evaluated. Design constraints surrounding the coil design are identified from this evaluation. A new solution is proposed, taking into consideration the identified constraints and demonstrating significantly improved performance. Results of FEM analyses are then experimentally verified and the performance of the solution is evaluated. Issues are identified surrounding localization of heating and the unsatisfactory response of the dissimilar metals to the applied frequency. This highlights the need for further investigations to be conducted.

In Chapter 4 an investigation is carried out through FEM modelling of the design of an appropriate electromagnetic flux concentrator. Additionally, the selection of an improved operational frequency is investigated and evaluated. The results of the FEM models are presented and their validity is discussed.

Chapter 5 concludes the Thesis with a summary of the investigations and findings, and suggests the future work..

Chapter 2

Literature Review

2.1 Introduction

In Chapter 1 the importance of flux concentration for induction coils used in applications requiring targeted heating was briefly discussed. In addition, the need for selection of an appropriate operating frequency was highlighted. These issues and those described with present methods of brazing used by Heat Treatments Ltd, have motivated investigation into the different methods of flux concentration and induction brazing. A literature survey of previous work in these areas, and those related to the application, is presented in this chapter. The literature review is divided into sections to consider specific aspects related to the fields of induction brazing, magnetic flux concentration and differing electro-thermal calculation methods. To the knowledge of the author, all recent work carried out in this area has been considered.

Section 2.2 describes the literature survey method used. Survey results are then tabulated and categorized by their field of relevance. In Section 2.3, the field of induction brazing is discussed and the relevant literature is presented. Section 2.4 documents recent literature in the field of electromagnetic field concentration. In Section 2.5 methods of electromagnetic field calculation and modelling are presented and discussed. Section 2.6 concludes the survey, highlighting the approaches to be applied from literature, and identifying the knowledge gap this Thesis will address. Section 2.7 presents the research methodology used in this Thesis.

2.2 Literature Survey Method

Three engineering data bases (IEEE Explore, Science Direct and Electrical Engineering Net Base), were used to find research that reported on induction heating and methods of electromagnetic field concentration. The search included articles published between 1990 and 2018. Only articles in English were searched. The search string used was (Induction heating OR flux concentration OR electromagnetic field concentration OR magnetic field concentration OR flux concentrator OR induction brazing) (NOT coil gun NOT motor NOT generator NOT machine). This search generated 969 results of which just 269 were deemed relevant according to their title. These documents were then sorted through and all duplicates were removed along with obsolete versions and irrelevant information leaving 80 papers. The remaining papers were then each briefly analysed for relevant information leaving 38 documents on which a full text review was carried out resulting in the exclusion of a further 9 papers. Further papers were found at a later date bringing the total up to 33. The remaining papers have been categorized and tabulated according to their field of relevance in Table 1. This research shall now be discussed.

Specific Area of Relevance	**Sub-topics**	**Reference ID Number**
Induction Brazing	Dissimilar metals, Fluxes and fillers/alloys, Frequency, Power, Eddy current penetration	[4] [5] [6] [7] [8] [9] [10]
Magnetic Field/ Flux Concentration	FEM analysis, Eddy current distribution, Mathematical field simulation, Coupled electromagnetic and thermal calculations, Induction coil design, Localized induction heating, Skin effect, and Current density.	[4] [5] [6] [11] [12] [13] [14] [15] [16] [17] [18] [19] [20] [21] [22] [23] [24] [25] [26]
Electromagnetic Field Calculations	FEM, Skin depth, Linear/ non-linear impedance calculations, Coupled electromagnetic and thermal calculations, Mathematical field simulation	[14] [19] [26] [27] [28] [29] [30] [31] [32] [33]

Table 1 – Categorized research topics

2.3 Induction Brazing

Approximately 75% of all brazing applications are accomplished with flame heating. The remaining 25% are satisfied by two other heating processes; induction and resistance heating [31]. The only method that will be discussed in detail in this Thesis is induction brazing.

2.3.1 Key Considerations for Successful Induction Brazing

When attempting to braze components it is important that an appropriate flux and filler material (also known as alloy) are selected so as to achieve a strong and uniform joint. Silver based fillers are used when joining ferrous and non-ferrous metals, although copper and copper-nickel fillers can also be used in most cases [34]. Brazing fluxes are used to protect the joint area from oxidation during the heating process so as to ensure good-quality brazed joints. The selection of a flux depends on the type of filler, the base material, and method of heating.

There are many important considerations to be made when attempting to induction braze materials, especially if they are dissimilar materials. Five key technical considerations include [10]:

- The thermal conductivity of materials to be brazed
- The thermal capacity of materials to be brazed
- The distance of work-piece from the inductor coil
- The operating frequency of the induction power supply
- The rate of heating

These will now be explained.

The thermal conductivity of a material is generally linked with its electrical resistance and is an expression of how easily heat can be conducted or transferred throughout a material [10]. Materials with greater electrical resistance have lower the thermal conductivity and vice versa. Thus, materials that have a high electrical resistance are well suited for heating via induction, as induced heat remains localized. Therefore, knowing the thermal conductivity of a material is helpful in determining whether or not it is suited to heating, or in this case, brazing via induction.

The thermal capacity of a body relates to the energy required to raise the temperature of that body by one degree. It is inextricably linked to the physical size as well as the material type. If this is not given sufficient consideration then the results can be a lack of control over the brazing process, or damage to the component(s), due to over-heating.

The distance between the work-piece and induction coil is critical in achieving effective and efficient brazing results. This is due to the fact that the induced heating in a work-piece is inversely proportional to its distance from the coil, as given by [10]:

$$h \alpha \frac{1}{r^2}. \tag{1}$$

Where, h = induced heating, and r = distance between coil and work-piece.

Therefore, if the work-piece is not correctly located inside, or below the work coil, then the area closest to the coil will experience greater heating than the rest of the component. This can result in localised over-heating with the brazing flux being burnt off in one area of the work-piece, allowing it to be oxidised, before the rest of the joint has reached brazing temperature.

The frequency of the power supply is also highly important to consider. The density of the induced eddy currents is greatest at the surface of the work-piece and the current density decreases towards the center of the component. This phenomenon is known as the skin effect. The skin depth is the distance from the surface of the material to the depth where the induced field strength and eddy currents are reduced to 37% of their surface values [9]. The frequency at which an induction heating system operates determines the eddy current penetration depth. Higher frequencies result in shallower heating depths and are often used for surface hardening applications. Lower frequencies result in greater heating depths as eddy currents penetrate deeper within the material (Fig. 2). However, it is important to note the fact that this penetration depth varies with temperature, due to the changes in material resistivity and permeability [35].

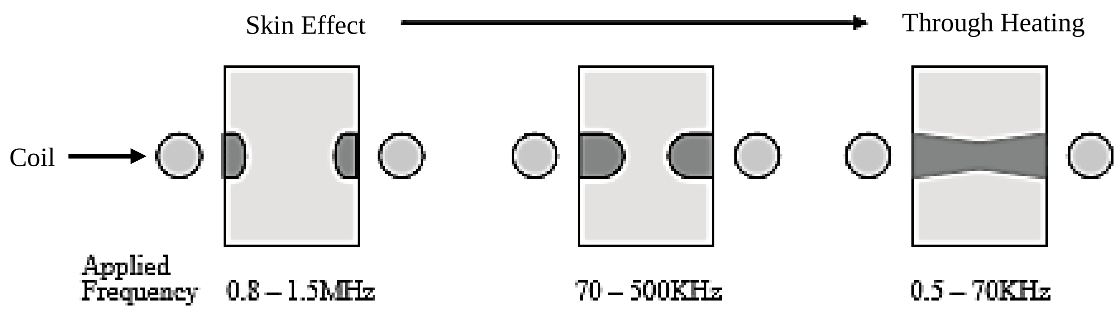

Fig. 2 – Effect of frequency on depth of penetration [10]

Calculation of the skin depth (δ) can be achieved using [17]:

$$\delta = \sqrt{\frac{2 \times \kappa_0}{\omega}} \tag{2}$$

Where, δ is the skin depth (m), ω = frequency (Hz), and the magnetic diffusivity (κ_0) is given by:

$$\kappa_0 = \frac{1}{\mu_0 \times \sigma} \tag{3}$$

Where, σ = electrical conductivity (S/m), and $\mu_0 = 4\pi \times 10^{-7}$ (H/m).

The average heating power that can be deposited within a depth (x) is given by:

$$\overline{P}_R(x) = \pi \mu H_0^2 \delta \left[1 - e^{-2x/\delta}\right], \tag{4}$$

Where: $\mu = (\mu_0 \mu_r)$, and H_0 is the magnetic field strength (A/m).

Given a sinusoidal magnetic field, the ratio of the mean heating power deposited within a depth (x), over a given time interval, $\overline{P}_R(x)$, to the mean heating power over the thickness of a work-piece to be heated, $\overline{P}_R(\infty)$, is given by:

$$\frac{\overline{P}_R(x)}{\overline{P}_R(\infty)} = 1 - e^{-2x/\delta} \tag{5}$$

From this it can be shown that [6] [17] [35]:

$$\overline{P}_R(\delta) = 0.865 \overline{P}_R(\infty) \tag{6}$$

Thus, it is apparent that most heating power (86.5%) over a particular time frame is concentrated within one skin depth. Therefore the operational frequency of the induction heating system should be such that the resultant δ is greater than or equal to the required depth of heating.
While heat transfer occurs through thermal conduction, thermal time constants mean that particular regions of an object can be effectively heated to high temperatures, before heat is transferred. This allows for heating to be localized to a desired region [17].

The rate and level of power input into the work-piece corresponds to the intensity of the generated magnetic field at the output inductor. The higher the input power, the greater the magnetic field and, consequently, the faster the rate of heating experienced by the work-piece. Therefore, due to the changes in material resistivity and permeability that occur with increasing temperature, the level of power input required will depend upon the application and its specifications. Thus, when selecting an induction power supply it is important that these factors are taken into consideration. For the power supply to be appropriately sized, an estimate of the necessary time frame for heating is required, so as to approximate the power required to heat the work piece. The following load power approximation can be used [9]:

$$P_1 = mc\Delta T \tag{7}$$

Where: m = mass (g) to be heated, c = specific heat of material, and ΔT = the change in temperature required.

To determine the total input power needed from the source, the power lost from the work piece, due to radiation and convection, and the loss in the coil itself, due to Joule heating, must be added to P_1. Heat loss due to convection is usually small and can be neglected in calculations for rapid heating applications. The following equation accounts for the radiation losses.

$$P_2 = Ae\sigma(T_2^4 - T_1^4) \tag{8}$$

Where e = emissivity of work piece surface (typically around 0.8 for oxidised steel, [9]), σ = Stefan Boltzmann constant ($W \cdot m^{-2} \cdot K^{-4}$), T_1 and T_2 = work-piece and ambient temperatures (K), and A = surface area of work piece (m^2).

The power loss in the induction coil depends on the frequency, coil design, and the size of the air gap between the inductor and the work piece. This can be approximated by:

$$P_3 = I_c^2 R_c \tag{9}$$

Where, I_c = coil current (A), and R_c = AC coil resistance (Ω).

At low frequencies (50-60Hz), R_c is approximately equal to the dc resistance value. However, at higher frequencies, a skin effect is also set up in the coil, and should be considered [9]. From these definitions, the total power required is therefore:

$$P_T = P_1 + P_2 + P_3 \tag{10}$$

The overall heating efficiency is given by:

$$\eta_H = \frac{P_1}{P_1 + P_2 + P_3}. \tag{11}$$

This efficiency is defined for the work-piece and coil only and does not allow for the losses of the power supply.

Observation of these five key considerations should result in a successful and efficient brazing process. For the application of this Thesis, the considerations described are of high importance due to the shielded nature of the brazing region and the dissimilar materials that are to be brazed. The effects of coil to work-piece distance, and operating frequency are of particular interest.

2.3.2 Brazing Applications

The most common applications of induction brazing with tungsten-carbide and steel are in the brazing of saw teeth, drilling bits, grippers, steel shanks, surgical devices, and cutting tools. Whilst there are many applications that make use of induction for the brazing of tungsten-carbide, the nature of the joint required to be brazed in this study is unique. Most applications such as the brazing of saw teeth are carried out at frequencies over 50 kHz. This is due to the fact that multiple faces of the part are accessible for the coil (Fig. 3), so shallow heating can bring the joint up to temperature. The tungsten-carbide inserts required to be brazed into 1020 mild steel jaws in this study are seated inside a slot in the 1020 mild steel bulk with the filler material beneath. Therefore, sufficient heating must be applied to the base of the slot and insert for successful brazing to result. Given the differing material properties of 1020 mild steel and tungsten-carbide this presents a significant challenge. One documented example of a similar application seen in Fig. 4, resolves this issue by simply heating the whole work-piece up to brazing temperature over 2 and a half minutes using a high frequency supply (see Appendix A) [3]. This provided a significant time saving and increased efficiency over the previous flame brazing method that was employed in [3]. However, this approach is still time consuming and electrically inefficient. The present furnace brazing method employed by Heat Treatments can process 60 jaws in approximately 4 hours, equating to one jaw every 4 minutes. Thus, for the induction brazing system to result in improved efficiency, a targeted heating approach must be taken, rather than heating the whole jaw up to brazing temperature. Due to the contour of the jaws to be brazed, this presents a significant challenge.

In addition to this, consideration must be given to how the field interacts with the parts to be joined, due to their differing material properties and electrical resistances. Therefore, the positioning of the coil with respect to the components should be such that it promotes even heating of the 1020 mild steel and the tungsten-carbide so as to avoid a faulty braze or fracturing of the inserts during cooling. Additionally, methods of field concentration should be applied to the coil. To the best of the author’s knowledge, an application of this unique nature has not previously been reported on.

Fig. 3 – Close up of saw teeth showing that multiple faces of the brazing joint are accessible to a coil [36]

Fig. 4 – Induction brazing of part using high frequency supply and un-targeted heating [3] (see Appendix A)

2.4 Electromagnetic Field Concentration

2.4.1 Field Concentration Methods

To achieve localised heating it is necessary that the magnetic field is concentrated to the desired regions to be heated and brazed. Materials that reduce the reluctance of the path for the magnetic field in induction heating systems are called magnetic flux concentrators [2]. These concentrators have three traditional functions in induction heating, the first of which being that they provide localised heating of chosen areas. They also act as an electromagnetic shield, preventing or reducing undesired heating of nearby electrically conductive regions [8]. Through the conducted literature survey, several methods of electromagnetic field concentration have been identified and are presented in Table. 2. The advantages and disadvantages of each will now be discussed, with respect to the industrial nature of the application under focus.

Table 2 – Methods of electromagnetic field concentration

Method	Explanation of method	Limitations	References
Field concentration via multiple Tx coils	This method uses several current controlled transmitting (Tx) coils to achieve concentration of the electromagnetic field. "*Ten Tx coils spaced 5cm apart with a 90cm-long ferrite core was fabricated. Magnetic flux of 1.5μT was centralized within a focusing resolution of 12.5cm at a distance of 10cm from the Tx coil, which is four times that of a non-focusing coil.*"	The use of multiple coils and multiple current sources would incur greater cost than other methods. In an industrial environment the use of multiple coils would be viewed as impractical.	[24]
Helm-Holtz coil pair	By adding one or more coaxial current loops to the original one, the axial magnetic field can be modified according to special requirements. The coil separation determines the field shape and concentration. The Helmholtz coil pair is defined by: $2l = a$. (l = distance between coils, a = radius of coils)	When the separation of the coil pair is larger than the radius, $(2l > a)$, the central field is at a minimum. The opposite is also true that at $2l < a$, the maximum field is obtained. Thus this method is limited by the coil radius and separation.	[6]
Multiple concentric coils	Multiple coils are inserted concentrically inside each other. Each coil is supplied from a separate inverter operating at the same frequency so as to achieve a uniform heating pattern.	This method is only suited to applications such as a heating plate or similar scenario where the work-piece is largely flat.	[12]
Field concentration via the use of Ferrites and MDM's	Ferrite pieces and magneto dielectric materials are used to concentrate the magnetic flux onto the desired regions, resulting in greater efficiency and faster heating.	Ferrite pieces must be designed specifically for the application, taking into account the saturation levels.	[15] [16] [17] [18] [19] [20] [21] [22]

Research carried out in [24] documents the focusing of magnetic fields using several current controlled transmitting (Tx) coils for wireless power transfer (WPT) (Fig. 5). In this approach, ten evenly distributed Tx coils spaced 5cm apart with a 90cm-long ferrite core was fabricated. Magnetic flux of 1.5μT was centralized within a focusing resolution of 12.5cm at a distance of 10cm from the coil, which is four times greater than that of a non-focussing coil. It can be observed that a significant focusing effect is achieved. However, the focused field is too wide and it magnitude too low for this approach to be suitable for induction heating.

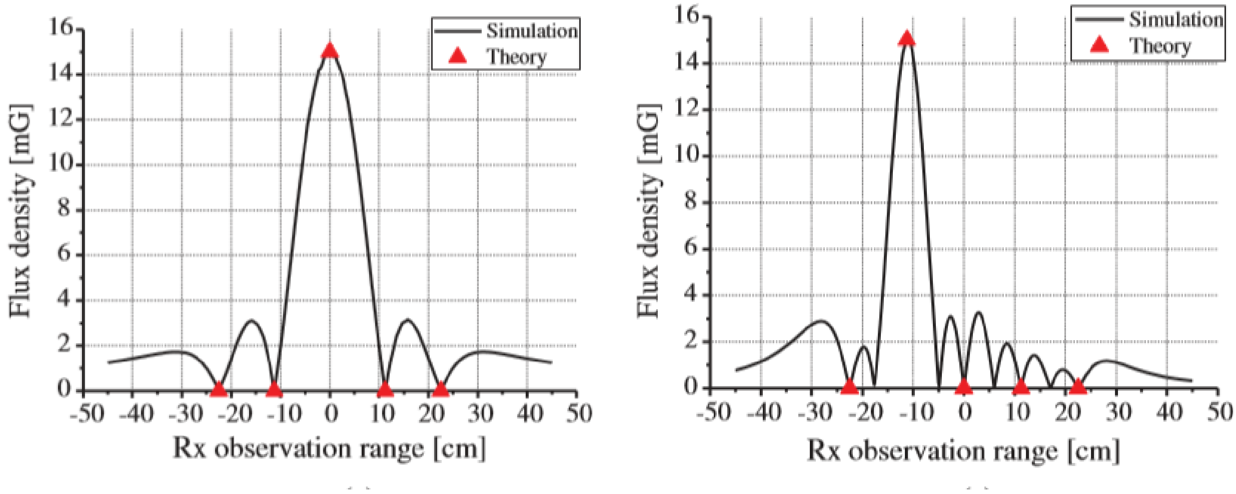

(a) **(b)**

Fig. 5 – Use of multiple Tx coils for magnetic field focusing, a) comparison of simulated and calculated results for the centralized flux density of 1.5 μT, (b) magnetic field focusing at Rx2, [24]

The results obtained are certainly noteworthy, however, due to the nature of the application in study, the use of multiple coils and multiple current sources would simply not be practical, or considered economically viable when compared to other existing methods. Therefore, this method shall not be studied any further.

The second potential method identified is referred to as the Helmholtz coil pair [6]. As briefly covered in Table 2, this method uses two or more coils to achieve a concentrated magnetic field via the polarities of the applied current sources to the coils and their relative spacing. It can be observed in Fig. 6 that both of the coils have their positive terminals at the top resulting in the field shape displayed. Switching the polarity of one coil around would result in a very different field shape.

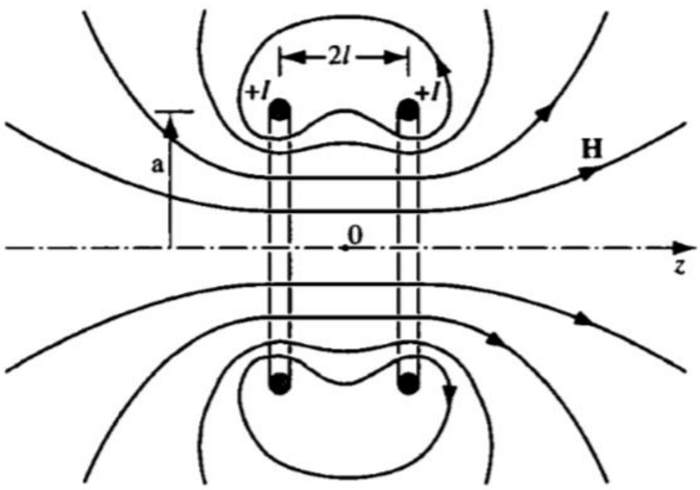

Fig. 6 – Helmholtz coil pair [6]

This coil configuration is best suited to applications in which the whole work-piece is required to be heated, due to its centralised field. However, by changing the length, *l*, between the upper and lower conductors independently, the field can be shaped to follow a curved path. For the application of this study, this method would not be an optimal solution, as targeted heating of only one region of the work-piece is required.

The next method identified is the use of multiple concentric coils [12]. Each of the coils is supplied from a separate inverter operating at the same frequency, so as to achieve a uniform heating effect (Fig. 7). This allows for the field magnitude to be increased in some areas over others resulting in the ability to heat contoured surfaces to a limited extent. However, this approach is primarily suited to applications in which the surface to be heated is flat such as a stove top application.

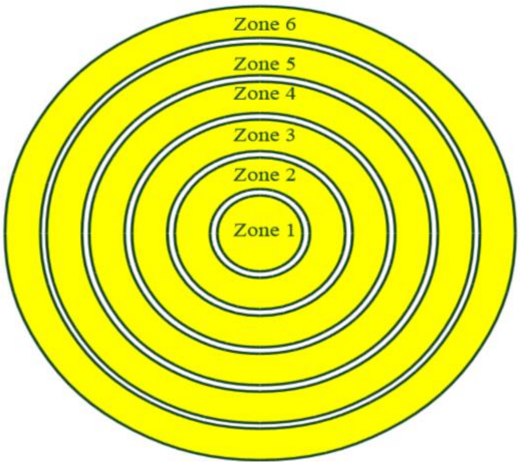

(a)

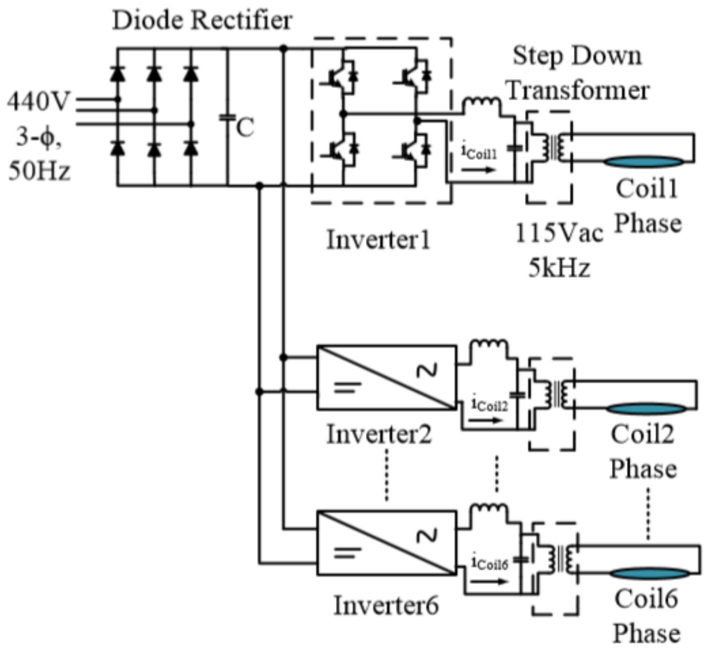

b)

Fig. 7 – a) Multiple concentric coils, b) power supply with multiple inverter stages for each coil [12]

The use of multiple supplies and coils is complex, and therefore would require skilled personnel to set up. Thus, this would simply not be practical or cost effective when the coil may need to be changed multiple times each day. Due to the power supply that is required, this approach is not well suited to the industrial application of this study. Whilst the field generated can to a limited extent be shaped to match a contoured surface, the contour of the parts to be heated is outside of this range. Therefore, no further investigation shall be made into this method.

Another method identified involves the design and use of ferrite pieces so as to achieve concentration of the electromagnetic field. Ferrite is a magnetic material commonly used as the core material for inductors and transformers. It has a high magnetic permeability and a low electrical conductivity, which results in minimal eddy currents under magnetically excited conditions. Examples of this method being applied from the literature reviewed include rice cookers (Fig. 8), barrel heating, rifle cartridge annealing, stovetops and more [15] [16] [17] [18] [21] [25] [29].

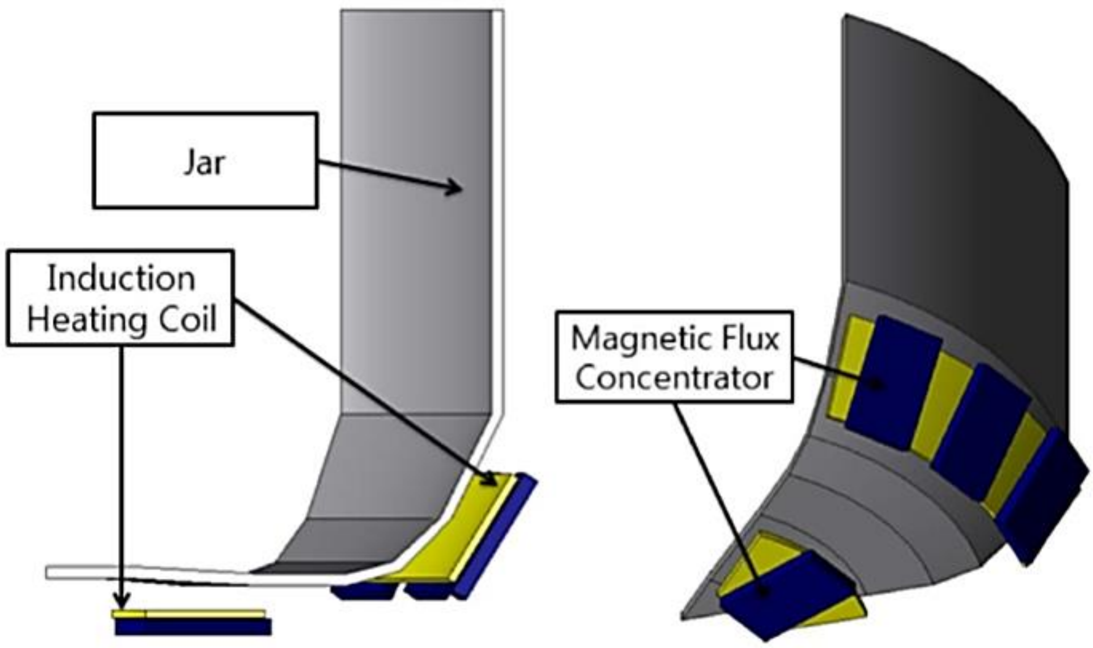

Fig. 8 – Use of ferrite pieces for flux concentration in rice cooker [18]

The benefits of this approach to field concentration are that:

- existing coil geometries can still be used in most cases, saving further costs
- the ferrite concentrators take up minimal space in comparison to other approaches identified by this survey [6] [12] [24]
- the ferrite can be custom made (at a cost), for the specific application
- Powder cores and machinable ferrites can also be used
- Less complicated and bulky than using laminated steels such as those used in transformers

The limitations of this approach relate to the saturation levels of the ferrite material and that excess heat can cause failure of the ferrite.

Magneto dielectric materials (MDM's) are soft magnetic materials that can be moulded to any desired shape or contour. This presents a significant advantage over other methods in that this type of product removes the need for computer design and machining as is often required for standard ferrites if they are not standard parts. One such a material is that of Fluxtrol Alphaform LF [37]. Similarly to standard ferrites, excess heat can cause a failure of the ferrite or MDM. Thus, the radiant temperature of the heated work-piece must be considered and appropriate heat shielding or cooling applied to the coil and concentrator, if this approach is used.

The field concentration approach to be applied in this study is that of magneto-dielectric materials. This is due to the fact that this approach will give the greatest flexibility in design and good field concentration, whilst also improving the electrical efficiency [22] [2]. To further this, the other methods identified, besides the use Helmholtz coils and ferrites, cost substantially more to develop and employ than that of MDM's. If any unexpected issues are met in the use of this material, ferrite pieces shall be used. Thus, all other identified methods are deemed either unsuitable or impractical for the industrial application of this study.

Induction coils are manufactured in many different shapes and configurations depending on the application. The number of turns required also varies greatly from one application to another, as this has a large effect on the current draw and field produced. One example of this from literature is that of inductive power transfer (IPT) coils for wireless charging of electric vehicles [21]. Fig. 9 depicts both rectangular and double-D winding configurations. The coils used in this application are made of litz-wire which is not suitably robust or heat resistant for application in induction heating systems. Additionally IPT coils are designed to generate fields over larger distances than are desired for induction heating applications. Therefore, this approach is not applicable for the application of this Thesis and shall not be further investigated.

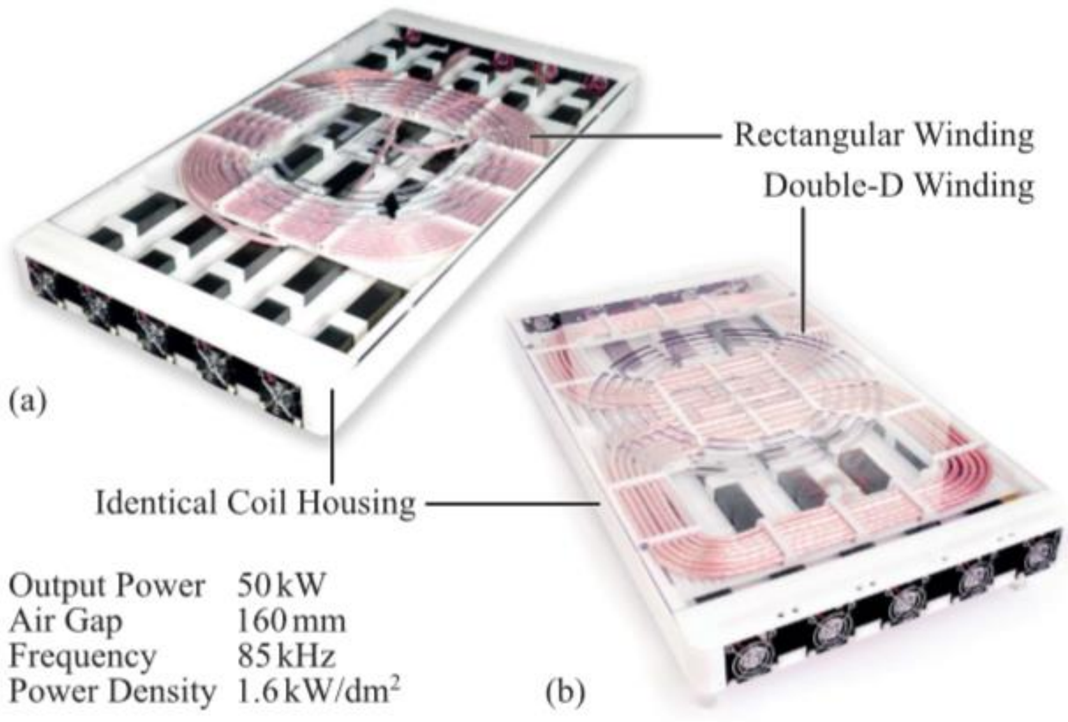

Fig. 9 – Rectangular and Double-D coils for IPT [21]

Induction heating coils can be classified into two families based upon the relationship between the magnetic flux direction and the part surface, longitudinal or transversal inductors. Longitudinal inductors generate magnetic field with lines flowing along the main axis of the work-piece. The field lines are perpendicular to the main axis of the work-piece for transversal ones [2]. When designing a coil for the purpose of induction heating, the number of turns and coil geometry is directly linked to the shape, size, and heating required (surface or through). For example, a cylindrical steel pin requiring surface hardening would typically have a single turn coil that encircles the work-piece [2]. If the part area required to be heated is circular and the surface flat, a multi-turn pancake-style inductor is generally the best suited approach [2]. The number of turns used in a coil is directly linked with the current flowing through it. Therefore, if the flux is desired to be held constant but the supply current reduced, the number of turns can be increased proportionally to achieve the desired reduction in current.

The coil designs suitable to be applied in the application of this research are only those of single turn coils. This is due to the specific nature of the region required to be heated and the contour of the work-piece which inhibits the use of multi turn coils. Therefore, any desired reduction in supply current levels can only be achieved by improved field concentration and coupling of the coil and work-piece, resulting in increased efficiency.

2.5 Calculation Methods:

This section discusses some of the relevant methods currently reported for the calculation of electromagnetic problems.

2.5.1 Electromagnetic & Electro-Thermal Calculations

The Biot-Savart law enables the calculation of magnetic flux density at the center of a circular coil and can be adapted for coils of rectangular geometries. [38]

$$|dB| = \frac{\mu_0 I}{4\pi} \times \frac{\sin\theta dx}{r^2} \text{ (T)} \tag{12}$$

Using the Biot-Savart law and integrating it over a current loop enables the calculation of the magnetic flux density, B, at any point in space around a coil as depicted in Fig.10.

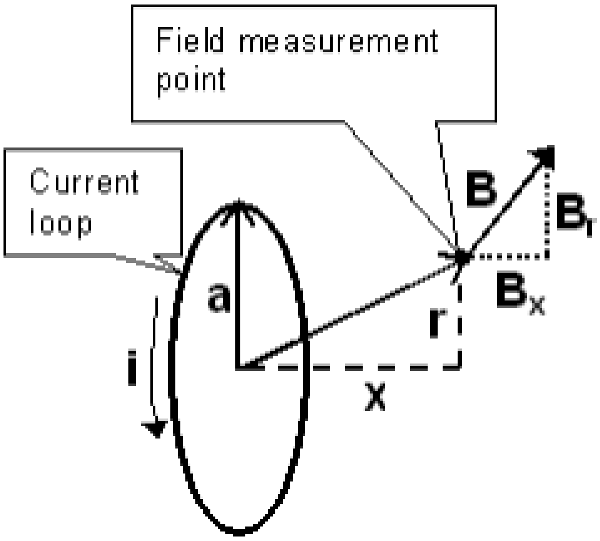

Fig. 10 – Calculation of B-field at a point in space [38]

Calculation of B can be carried out as follows.

$$B = B_x + B_r \text{ (Tesla)} \tag{13}$$

Where:

$$B_x = B_0 \times \frac{1}{\pi\sqrt{Q}}\left(E(k)\frac{1-a^2-\beta^2}{Q-4a} + K(k)\right) \quad \text{(Tesla)} \tag{14}$$

$$B_r = B_0 \times \frac{\gamma}{\pi\sqrt{Q}}\left(E(k)\frac{1+a^2+\beta^2}{Q-4a} - K(k)\right) \quad \text{(Tesla)} \tag{15}$$

$$B_0 = \frac{\mu_0 I}{2a} \text{ (Tesla),} \tag{16}$$

and where:

$$\alpha = \frac{r}{a} \tag{17}$$

$$\beta = \frac{x}{a} \tag{18}$$

$$\gamma = \frac{x}{r} \tag{19}$$

$$Q = [(1+\alpha)^2 + \beta^2] \tag{20}$$

$$k = \sqrt{\frac{4\alpha}{Q}} \tag{21}$$

Where, r = distance of point off of coil center axis (m), a = coil radius (m), x = distance from coil along coil center axis (m), K(k) = the complete elliptic integral function of the first kind, and E(k) = the complete elliptic integral function of the second kind.

This method is appropriate when the field strength is desired to be approximated at a point in free space. However, for the application of this study it is required that the field strength is approximated at points on the surface of the work-piece. This requires the use of an equation that accounts for the differing relative permeability's of the work-piece components and any flux concentrators applied to the work-coil, as demonstrated in Fig. 11. One such approach that can potentially be applied to this application is that of calculating the inductance, flux and field strength of air gapped inductors (Fig. 12). A standard approach is first covered below.

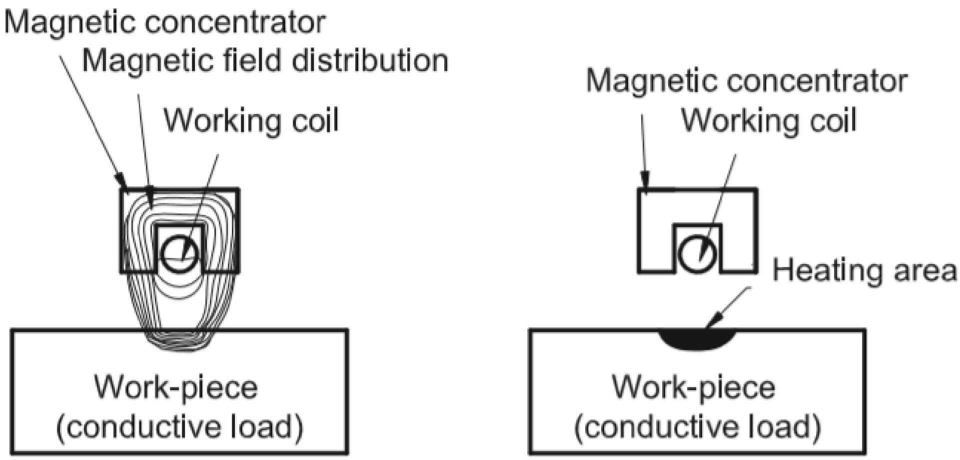

Fig. 11 – Flux concentrator applied to coil [16]

The current flowing through the winding sets up a magnetic flux that flows through the magnetic core and passes across the air-gap. The magnetic flux present remains the same in both the air-gap and the magnetic core material. The magnetic flux in the core can be determined by calculation of the path reluctance in the material and in the air gap. This model is only an approximation and does not account for leakage flux present in a real system. Fig. 12 depicts a basic model of this air gapped inductor which is similar to having an induction coil with a ferrite flux concentrator around it, as per Fig. 11.

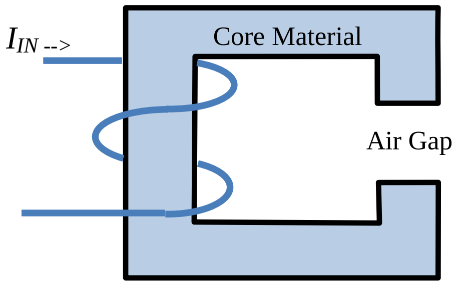

Fig. 12 – Air gapped inductor example

A more complex approach has been documented for the analysis of magnetic systems and magnetic equivalent circuits [14]. This approach attempts to account for the leakage flux present in a real-world scenario. The model presented illustrates a physical inductor as a magnetic equivalent circuit and proves a method of calculation, which accounts for the fringing flux present (Fig. 13). The method involves placing nodes throughout the inductor core cross section and calculating the Permeance (1/R) between each node.

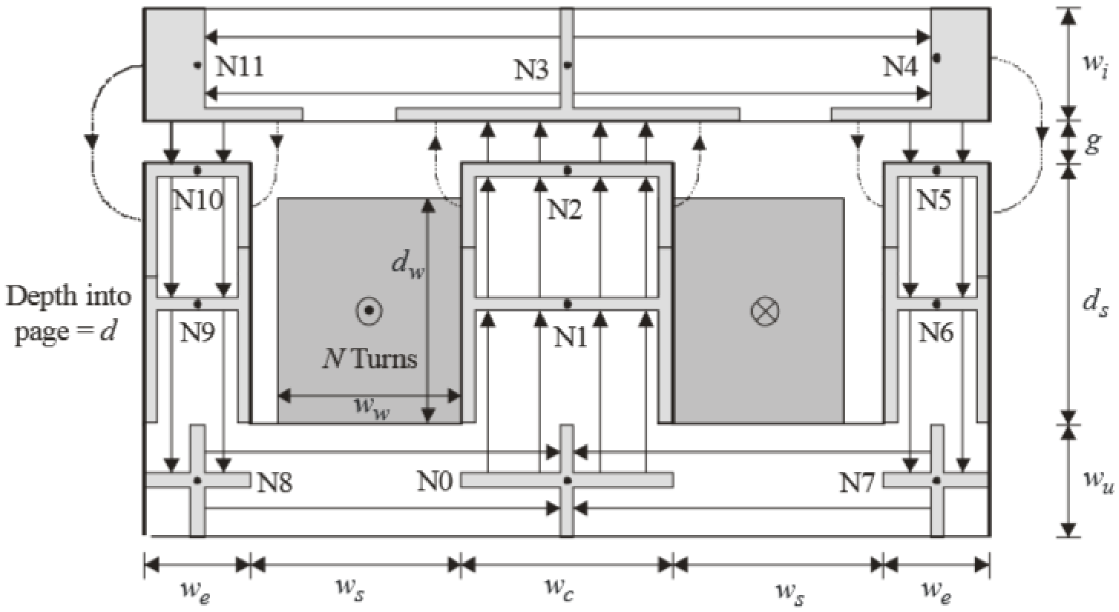

Fig. 13 – Nodal model of an EI cored inductor [14]

This approach accounts for the leakage flux in and around the core, and across the air gap, by including the leakage permeances in the magnetic equivalent circuit (Fig. 14). The circuit includes P_{vl}, P_{vb}, P_{hl}, P_{hb}, and P_f, denoting vertical slot leakage permeance, vertical bypass permeance, horizontal leakage permeance, horizontal bypass permeance, and face permeance respectively. This calculation method is better suited to the application of this Thesis, providing greater accuracy in the modelling of the flux density within the material regions, and accounting for the loss generated by fringing flux present in practical applications. However, the level of complexity presented in this analytical approach can result in a loss of insight. Furthermore, with the necessity of achieving localized, even heating, and an analytical approach enabling visual analyses of induced fields would be of greater value than that on a purely numerical basis.

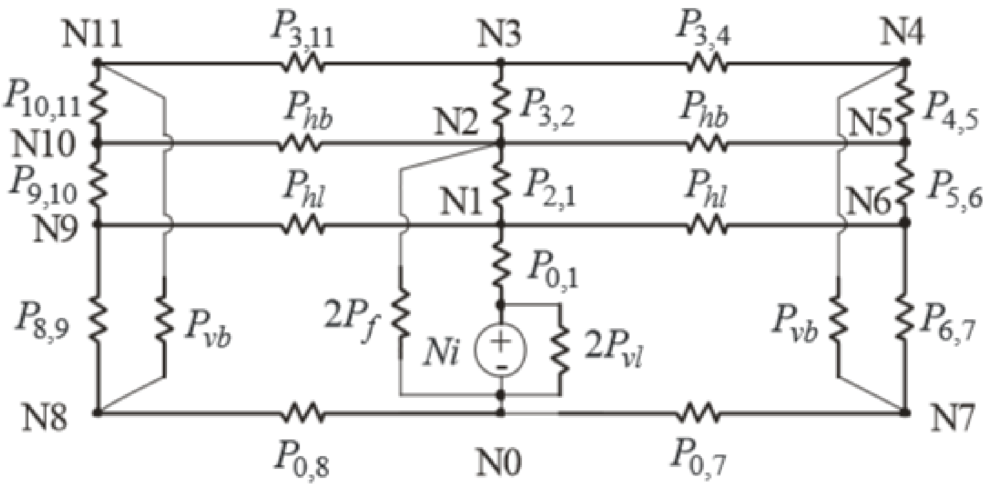

Fig. 14 – EI cored inductor modelled as a magnetic circuit [14]

Modern computer modelling is capable of accurately simulating complex electromagnetic and thermal phenomena in just a matter of hours (or less) [8]. In the field of electromagnetic induction heating, this has enabled the prediction of how different, interrelated, and nonlinear factors may influence the transitional and final thermal conditions of the subject material. This facilitates the rapid improvement of process efficiency and reduction of process development times, with less likelihood of unexpected practical outcomes.

One example from literature in which FEM modelling is used for analysis of an induction heating application is that of rifle cartridge annealing [17]. It can be observed in Fig. 15 that the eddy current density induced in a rifle cartridge is able to be visually analyzed. This enables performance to be critically evaluated as regions of higher or lower current density are able to be identified via simulation and adjustments made to achieve the desired results, before practical implementation. This can enable the reduction of development times.

Therefore, the FEM shall be applied in this Thesis. The software package to be used is that of ANSYS Maxwell.

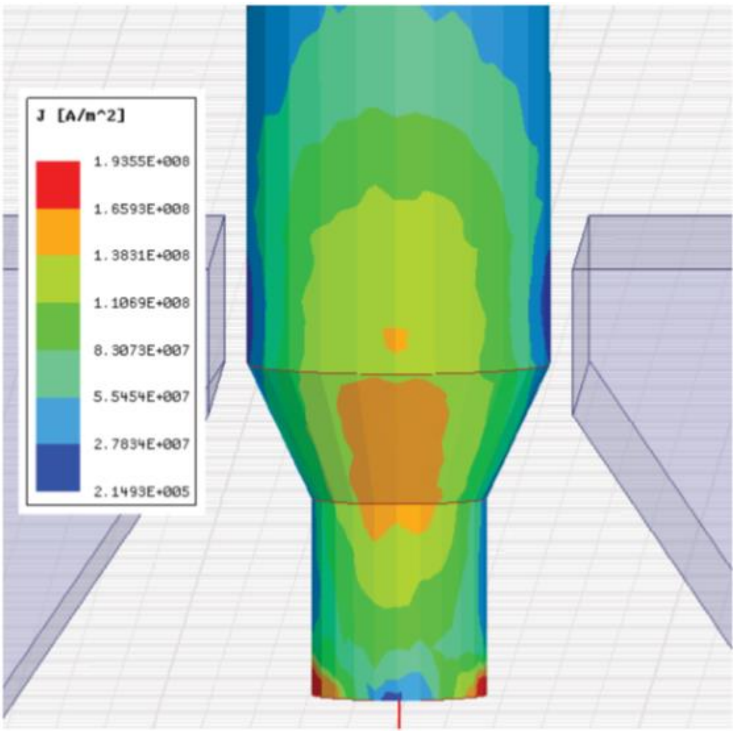

Fig. 15 – Induced current density with tapered ferrite poles [17]

2.6 Summary

This chapter presented a literature review of previous work undertaken in the fields of induction brazing and electromagnetic field concentration. Section 2.2 presented and discussed the survey method adopted in this study. In Section 2.3, the review of relevant literature and documentation in the field of induction brazing has identified the criterion for successful brazing. Furthermore, the survey conducted identified only one other study that considered the heating of regions that are shielded on all sides. The technique described is very inefficient. Therefore, a sufficient research gap is identified to warrant further investigation.

Section 2.4.1 discussed the topic of electromagnetic field concentration, identifying the most suitable method to be applied in this study. It was concluded field concentration through utilising MDM's best suits the application described in this Thesis. These materials are readily available for purchase and can be moulded or machined to suit the desired coil configurations. The topic of coil design was addressed in Section 2.4.2, highlighting the necessity of setting appropriate constraints (including supply current), to achieve desired outcomes. Section 2.5 presented several methods for the approximation of the B-field incident upon, and within the work-piece. It was determined that for the application of this research, a more suitable method of field analyses would be that of FEM. Following this, differing methods of computer modelling were briefly discussed and the FEM approach selected for use in this Thesis.

Therefore, Chapter 3 and Chapter 4 shall address the apparent knowledge gap identified by the conducted survey of recent and historic work in the field of induction brazing.

2.7 Research Methodology

Induction heating and brazing encompasses various aspects related to the physics of heating, magnetic phenomena, and material science. Accordingly, the research methodology accounts for these aspects, and the approach described below was used.

1. The modelling of induction brazing systems will be undertaken using the FEM. The models consider physical phenomena that include the effects of temperature on permeability, and resistivity, and the effect of frequency and resistivity on skin depth. In addition, the effect of Curie temperature on magnetic material properties will be allowed for.
2. Based on the modelling, design work on an improved induction coil design is possible, and such a design will be undertaken. It will consider practical issues and constraints that must be accounted for to allow for successful induction brazing and experimental validation.
3. Designs will be constructed, and performance verified experimentally. Verification will be in the form of comparison between FEM modelling results with the physically observed heating phenomena and resultant brazing quality.
4. Conclusions will be drawn.

Chapter 3

Development of an Improved Coil Design and Insert Retention Mechanism

3.1 Introduction

As discussed in Chapter 2, the induction heating requirements to achieve reliable brazing of inserts to jaws are complicated by the difficulty of getting heat to the brazing location. This difficulty arises because the surfaces to be mated are shielded on all four sides. Evidence on the problem this presents is apparent from knowledge that a commercial solution (purchased before development work by the author), resulted in failure, causing a safety issue. Modifications attempting to prevent this failure mechanism resulted in sub-optimal performance, as unreliable brazing and excessively long heating times resulted. This motivated research to design and develop a new coil to be used with the existing commercial power supply. The results of the research are presented in this chapter, and it is shown the induction brazing performance of the newly designed system is far superior. This research is undertaken through modelling the induction heating process using the FEM, in a manner that takes account of changes in the magnetic properties of materials in the approach to Curie temperatures. The results are validated experimentally.

Section 3.2 will discuss the work carried out to date by Heat Treatments, including the installation of a new induction heating unit. This section shall also discuss the results of FEM and physical analyses on the commercial unit. Section 3.3 will document the development of an improved coil design. The results of both FEM and experimental testing are also presented and discussed. Section 3.4 shall conclude the chapter and highlight any shortcomings.

3.2 Previous Induction Brazing Coil Attempts

In this section early attempts undertaken by Heat Treatments to implement an induction brazing system are presented. A commercial solution developed by Radyne Ltd [39], is also presented. It is shown that the performance of the Radyne coil is poor.

3.2.1 Initial Attempts by Heat Treatments

Initial induction brazing experimentation was carried out by staff at Heat Treatments using existing power supplies. Basic coils were formed out of copper tube as depicted in Fig. 16. These early trials often resulted in a meltdown of the induction coil due to insufficient cooling, long heating cycles, and poor coil design. Following this, research began into the design of an improved coil. A small power supply was hired so as to facilitate the development of new coils and a process for the successful brazing of the jaws.

Fig. 16 – One of the initial coil design attempts by Heat Treatments

One of the early attempts at designing a coil that could braze the jaws, without melting down due to the radiant heat exposure, can be seen in Fig. 17. It is evident that these early coils are by no means ideal for the application. The nature of the heating pattern generated from the rectangular coil, pictured in Fig. 17, will result in the entire mass of the jaw being raised to brazing temperature via thermal conduction. This is an electrically inefficient and time-consuming method of heating which, consequently, is also slower per jaw than the current vacuum furnace brazing method. The reasoning for trialling this approach was that previous attempts to design a coil that would sit above the jaw, as in Fig. 16, resulted in the coil melting down due to the long periods of exposure to the radiant heat from the jaw surface. However, this is only due to the poor coil design and selection of operating parameters. An appropriately designed coil, operated at the correct power and frequency levels for the application, would result in much shorter heating times and enable the use of a coil positioned directly above the jaw. Therefore, the decision was made to invest in a commercially developed system.

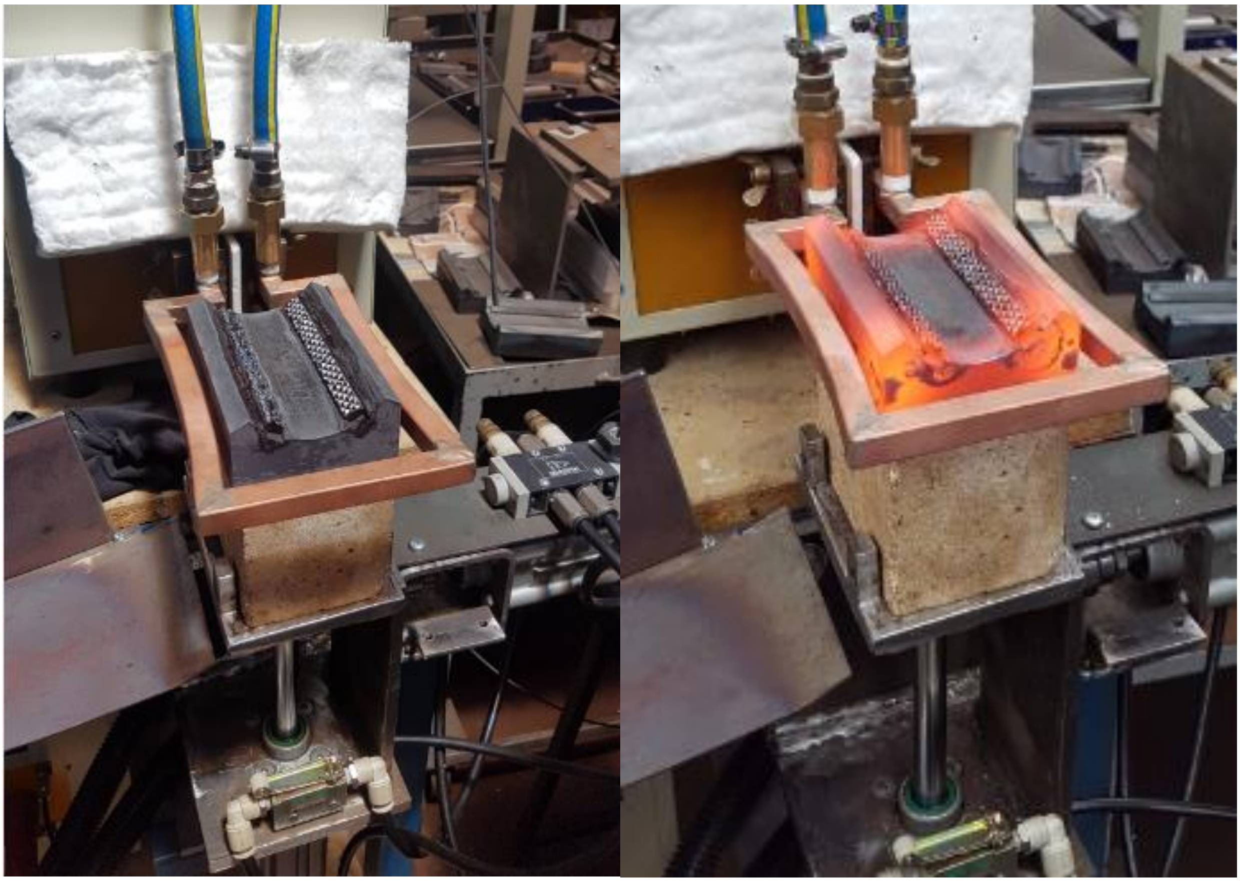

Fig. 17 – Rectangular coil design resulting in inefficient and slow heating

3.2.2 *Commercial Solution*

Induction heating systems are readily available for purchase. One such system was acquired by Heat Treatments from Radyne (Fig. 18). The machine was primarily purchased for the purpose of brazing, so as to enable a move away from the current furnace brazing method. Another reason for the move to induction brazing is the fact that induction processes are well suited to partial or full automation, enabling further increases in productivity [40]. Radyne were also contracted to design a custom coil that would enable the company to start production soon after installation (Fig. 19). The power supply is rated to supply 75 kW at a 10 – 30 kHz frequency range. Radyne recommended that for operation using their coil, the power supply should be set to 30% power, with 10 kHz supply frequency. However, during the first trial braze it became clear that several factors had been overlooked in the coil design. The first being that the tungsten-carbide inserts become attracted to the coil when it is energised. This resulted in failure, with the inserts jumping out of the slots and shorting the induction coil to the workbench. This presented not only a failure of brazing, but a significant safety issue. The workbench was suitably earthed; however it is not acceptable for this to regularly occur. The issue of the tungsten-carbide teeth jumping out of the slots had not previously been noted by Heat Treatments. This is due to the fact that all previous trials carried out with over-head coil configurations, had been on jaws that were already brazed by the furnace and simply required re-working. Thus, the inserts were held in place by the filler material.

Another issue noted was the inefficient heating pattern and resultant slow heating time. Testing carried out with the Radyne coil indicates that the field generated is poorly focussed and does not penetrate to desired regions. It can be observed in Fig. 20 (taken from a later trial) that the majority of heating occurs on the outer edges of the jaw. This means thermal conduction is relied upon to transfer heat to bring the slots and inserts to brazing temperature. The consequence of this reliance is slow heating times in excess of 1 and a half minutes, and localized overheating of portions of the jaw, resulting in decarburisation and scaling of the 1020 mild steel. After the trial it was evident liquation had occurred, as bare copper could be observed between the insert and the slot when viewing the jaw end-on [10]. This suggests the brazing may have resulted in a weak joint. Despite the poor design and clear lack of experimental work carried out by Radyne, the resultant heating time was improved over previous attempts by Heat Treatments. This however, is due to the selection of better operating parameters recommended by Radyne.

Fig. 18 – Radyne induction power supply

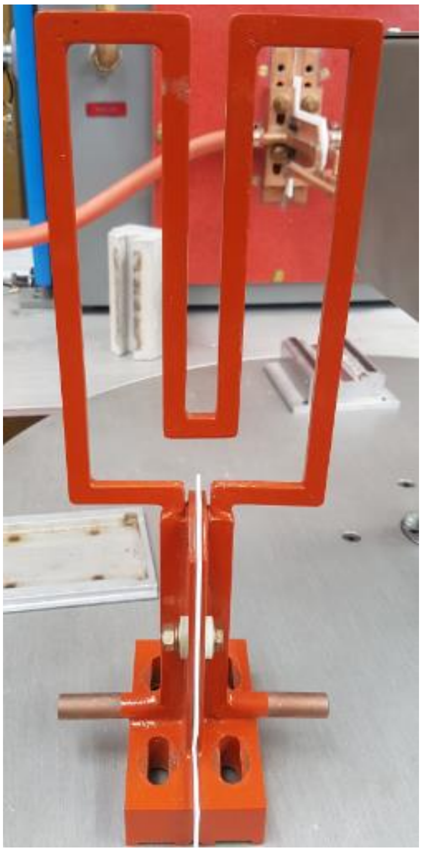

Fig. 19 – Radyne induction coil

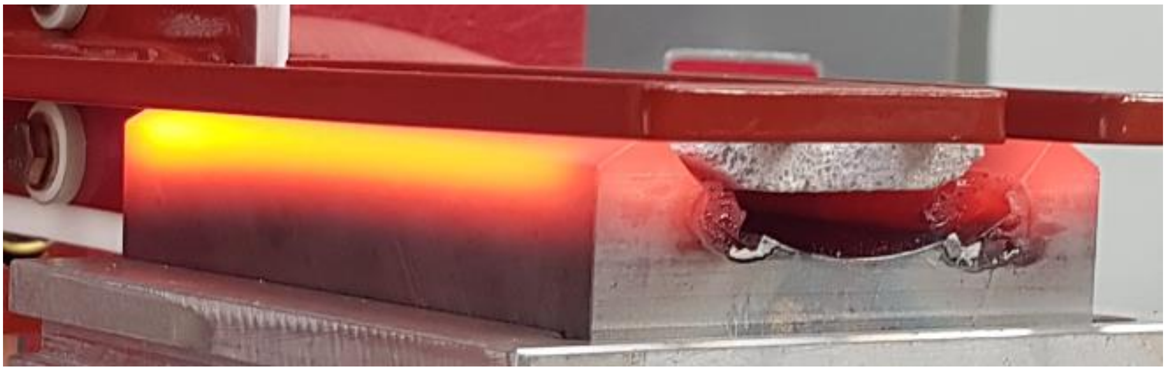

Fig. 20 – Brazing trial with Radyne coil

3.2.3 Theoretical Analysis of the Commercial Solution

Simulations of the coil produced by Radyne have been carried out in ANSYS Maxwell so as to analyse the field generated. The coil and jaw have been modelled in a 2D cross-sectional form and the B-field simulated. Table 3 contains material properties for both 1020 mild steel and tungsten-carbide which have been applied to the simulated models. Fig. 21 shows the FEM modelling results for this induction brazing coil placed over a jaw being heated at (a) 25 °C, (b) 500 °C, and (c) 770 °C, at 10 kHz, with simulated coil currents of 800 A. The 800 A coil currents are used as this is the practical output current when the supply is operated at 30% power. The 10 kHz frequency was used in this model as that is the lowest operating frequency of the Radyne power supply. For the models, the resistivity of tungsten-carbide and 1020 mild steel are assumed to increase in compliance to the temperature coefficient of resistivity's listed in Table 3. The result of this is changes in skin depth which, in the case of 1020 mild steel, are significant after changes in permeability are also allowed for. These properties are demonstrated in Fig. 22. To account for these variances in resistivity and permeability in the 1020 mild steel, the jaw in Fig. 21 (a), (b), and (c), has been segmented according to the skin depth at the given temperature, and the values of resistivity and permeability for the top segment have been changed accordingly. The sharp drop in permeability within the top segment is justified by the fact that 86.5 % of power deposited in a material through induction heating is concentrated within one skin depth [35] [6], which will cause localized heating and the Curie temperature of the 1020 mild steel being exceeded. The low thermal conductivity of 1020 mild steel limits the speed of heat transfer out of this localized region. For the model used at 25 °C, the skin depths of the tungsten-carbide and 1020 mild steel are low compared to higher temperature values, as permeability and resistivity are relatively high. This initially limits magnetic field penetration to shallow depths for both materials, as shown in Fig. 21 (a). Fig. 21 (b) shows magnetic field penetration improves at higher temperatures for the 1020 mild steel, as its magnetic diffusivity changes significantly. However, it can be observed that the field is not concentrated at the bottom of the slot for the tungsten-carbide insert. In effect the inserts act as a magnetic shield. This is because the Curie temperature for tungsten-carbide with a cobalt binder is approximately between 950 to 1,050 °C depending on the alloy composition [41]. Thus, the relative permeability of tungsten-carbide can be assumed to remain almost constant at temperatures from 25 °C to 770 °C. For the model used for 770 °C, the relative permeability of the 1020 mild steel is set to a value of 1 for a distance from the jaw surface equal to the skin depth, as it is assumed this region is at the Curie temperature. Beyond this distance the 1020 mild steel is assumed to have a permeability of 150, as the temperature is significantly lower than 770 °C. It can also be observed that the highest field strengths are present on the outer edges of the jaw and in the top of the tungsten-carbide inserts. Consequently, this system must rely largely upon thermal conduction to get the brazing metal filler to its melting temperature, given the lack of magnetic field penetration at the bottom of the slot. This is highly inefficient. The nature of the magnetic field in Fig. 21 (c) is similar to the heat distribution practically observed in Fig. 20 indicating agreement between experimental and modelling results and confirming the inadequacy of this system.

Table 3 – Material Properties – (see also Appendix B)

Properties	**Materials**	
	1020 Steel [42] [43]	***Tungsten Carbide – 10% impurity*** [44]
Resistivity (25°C)	0.159 μΩ/m	0.19 μΩ/m
Resistivity Temp. Coefficient	0.005	0.0045
Electrical Conductivity	0.62893×10^{7} S/m	0.526316×10^{7} S/m
Thermal Expansion	12 μm/m-K	6.5 μm/m-K
Density	7.872×10^{3} kg/m^3	15×10^{3} kg/m^3
Relative Permeability (25°C)	150 H/m (approx.)	12 H/m at 10 kHz (approx.)
Curie Temp.	770 °C	950 °C – 1050 °C [41]

This agreement confirms that new coil design ideas can be accurately modelled using the FEM, knowing that they will perform similarly in practice and reducing the time between developments. Given the unsatisfactory field distribution and resultant heating pattern observed through both simulation and experimentation, it is evident a new coil geometry must be developed. Unlike the commercially developed solution, the scope of the coil design must be expanded to include a means of insert retention, whilst providing a more targeted and uniform heating effect beneath and surrounding the slots. Therefore, the following sections report on the development of an appropriate solution to the identified issues with the present coils.

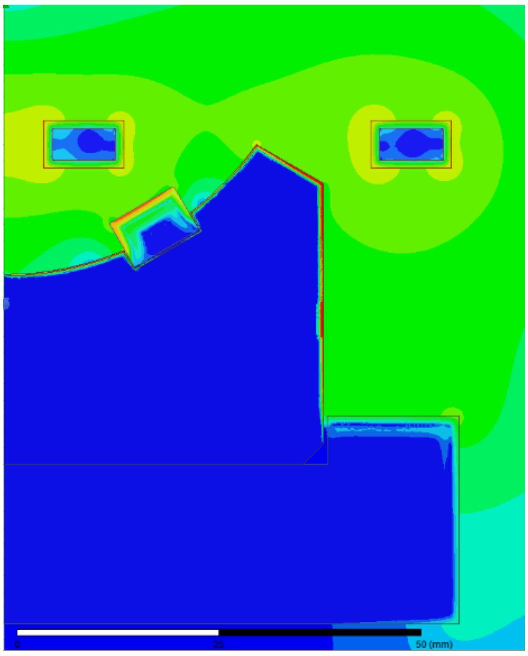

(a)

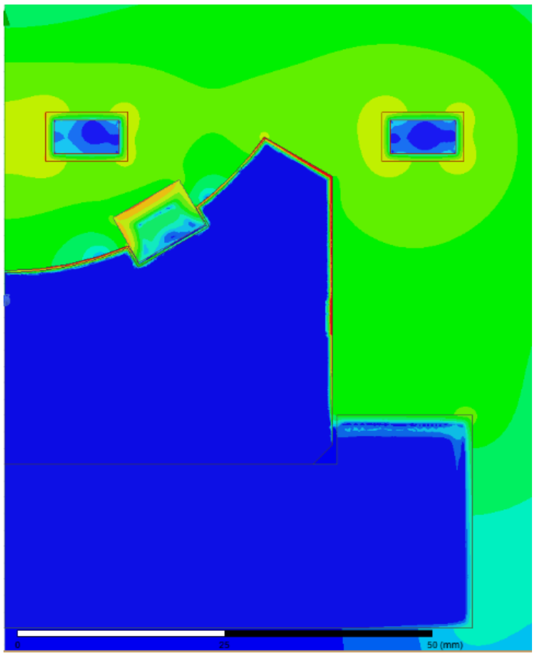

(b)

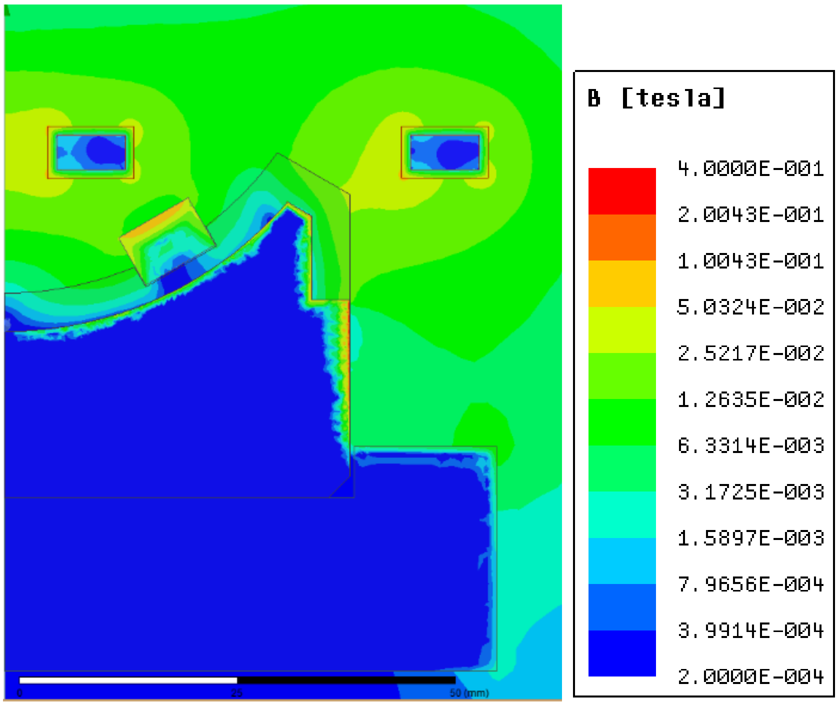

(c)

Fig. 21 – Magnetic field without guidance at 10 kHz (a) 25 °C, (b) 500 °C, (c) 770 °C

3.3 Development of an Improved Coil for Existing Power Supply and Identification of Coil Design Constraints

Testing carried out with the Radyne coil indicated that the field generated is neither concentrated, nor penetrating into the desired regions. This lengthens the heating time, as reliance is made on thermal conduction, and results in scaling of the work-piece. Additionally, as briefly discussed in Section 3.2.2, the inserts must be retained during the heating cycle. The addition of a retainer between the coil and the inserts restricts how closely the coil can be placed to the brazing regions. Therefore, a key design constraint is that the coil must allow sufficient access to the inserts from above. This restricts the possible geometries. Thus, the goal for an improved coil is to minimise, or eradicate scaling, through reducing heating time by targeting the magnetic field at the brazing region.

3.3.1 Improved Coil with Compliance to Design Constraints

Knowing that the frequency of operation determines the skin depth of heating, [6], it can be easily determined that the 10 kHz frequency in use is not ideal for the application, resulting in a skin depth of just 0.26 mm. This confirms the poor simulation results in Fig. 21. Fig. 22 clearly demonstrates this by plotting the skin depth vs temperature for tungsten-carbide and 1020 mild steel, and also shows the roll-off of permeability at Curie temperature for 1020 mild steel. However, given that the frequency range of this machine cannot be changed and significant investment has been made into its installation, an improved coil must be developed to suit this machine. Thus, developments documented in this chapter are by no means optimal, but are designed to suit the present apparatus.

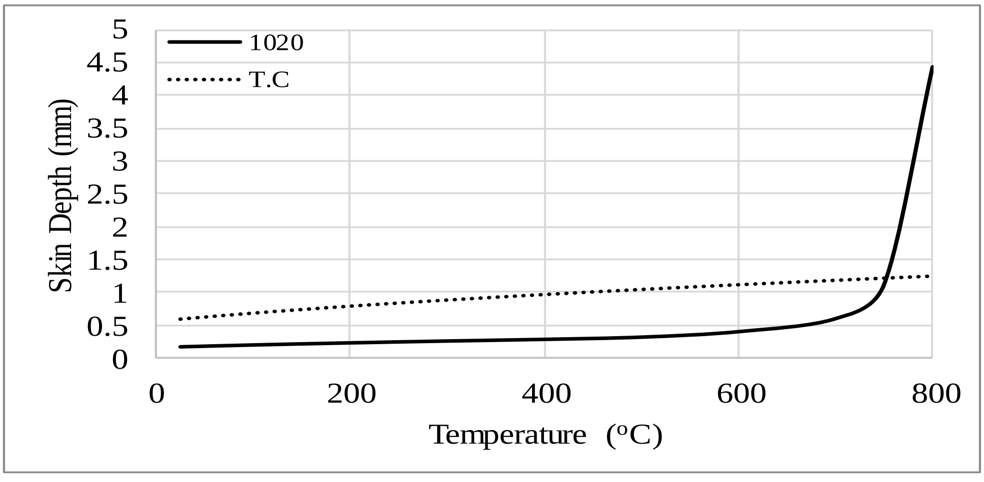

Fig. 22 – Skin Depth vs Temperature at 10 kHz

The existing Radyne "M" coil shape could be used. For this shape the magnetic field produced at the center of the coil is lowered. This is due to the opposing field directions produced by the center conductors and is supported by Fig. 23 [9] [45], and Fig. 24 (a) and (b). Whilst FEM modelling of the Radyne coil, Fig. 24 (a), shows that the magnetic field in the center is shaped to have a null, the resultant heating would be more efficient than that in Fig. 24 (b) with unidirectional current flow in the center conductors. This is due to the fact that there is a significant increase in the flux density in the center of the coil which will result in the entire surface of the jaw experiencing heating. The configuration of the Radyne coil, in theory, minimizes heating in undesired regions through the advantageous use of this null effect. However, due to the constraint caused by the need for insert retention, the distance between the coil and the jaw is not able to be reduced sufficiently for the benefits of this field shaping to be realized in practice. Hence, poor heating patterns are experienced. Therefore, to achieve greater flexibility in brazing jaws with differing pitch and slot spacing, whilst allowing sufficient clearance for an insert retention mechanism, the central conductors must have unidirectional current flow. As reported in [6], the electromagnetic field can be shaped to achieve a concentration effect via the use of the Helmholtz coil pair method. Therefore, an improved coil design may result with unidirectional current flow in the central conductors and vertically off-set outer conductors, so as to follow the curvature of the jaw.

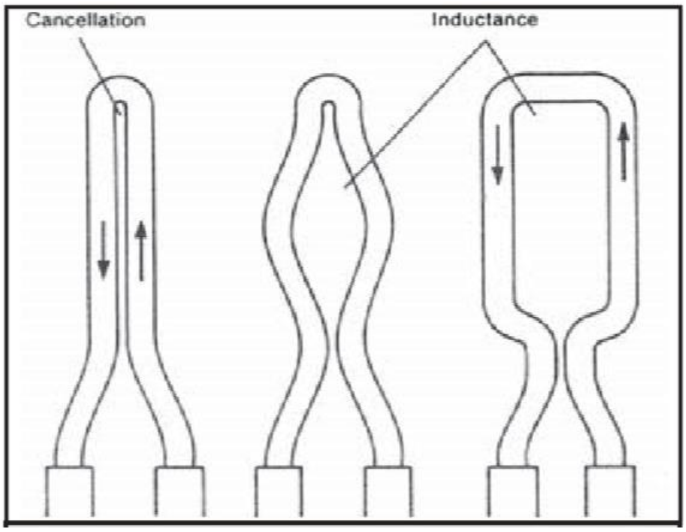

Fig. 23 – Effect of coil design on Inductance [45]

Simulations of one of the '8' series jaws have been carried out, so as to model the effectiveness of a coil using the Helmholtz approach to field shaping. The modelled coil has unidirectional current flow through the central conductors and vertically offset outer conductors with reversed polarity to the central conductors. This style of induction coil belongs to the family of transversal inductors, due to the work-piece orientation beneath the coil [2]. It can be observed in Fig. 25 (a), (b), and (c) that the field strength is much greater in the region surrounding the inserts than in the previous coil simulations. In addition to this, the field is more concentrated, resulting in less interaction with the outer surface of the jaw. Accordingly, it can be concluded that the heating effect resultant from this coil will be a vast improvement over the Radyne coil.

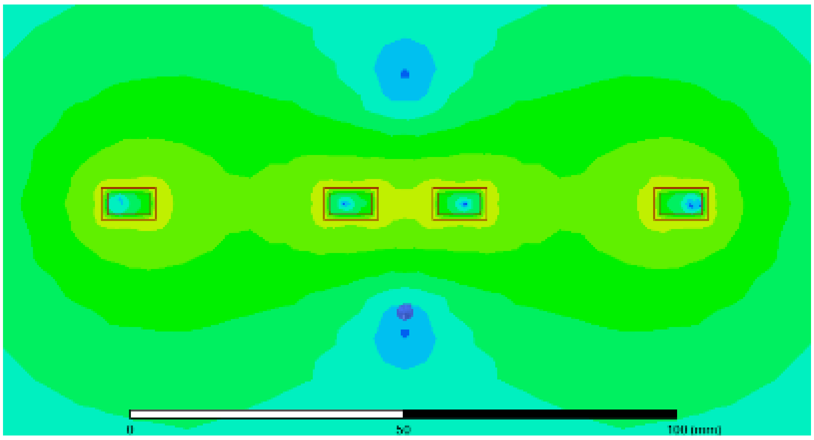

(a)

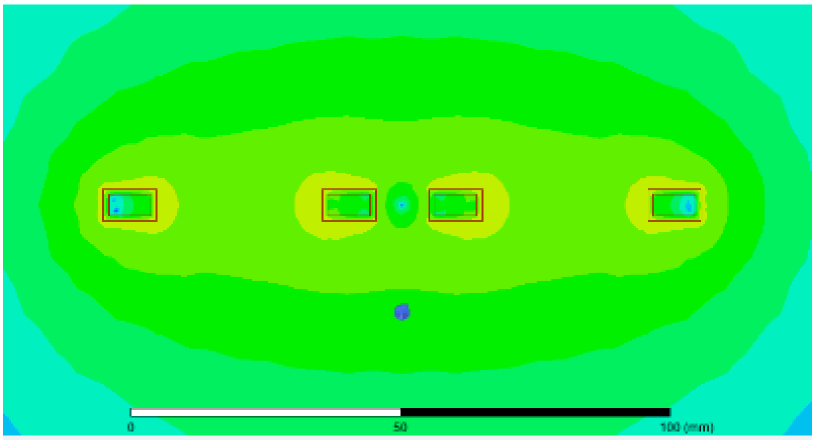

(b)

Fig. 24 – Effect of current direction on field shape of coil cross-section (a) "M" shape with (+ - + -) continuous current path, (b) unidirectional (+ - - +) current flow in central conductors

It can also be observed that offsetting the coil conductors to follow the contour of the jaw results in shaping of the field to follow the contour of the jaw. This in turn results in greater field strength present in the desired region beneath the inserts than that of Fig. 21 (c). This is due to the fact that the outer conductor is able to sit over the top of the jaw. Thus, the field is more centralised above the jaw, and is much weaker along the outer edge. Although improved, the field is still not concentrated effectively, as significant flux density is present in the areas surrounding the coil and jaw, especially for the initial state at 25 °C. Additionally, it can be observed in Fig. 25 (b), that the operating frequency of 10 kHz does not allow for full penetration beneath the inserts. There are two or more regions beneath the inserts in which there is little to no field strength, indicating a reliance on thermal conduction.

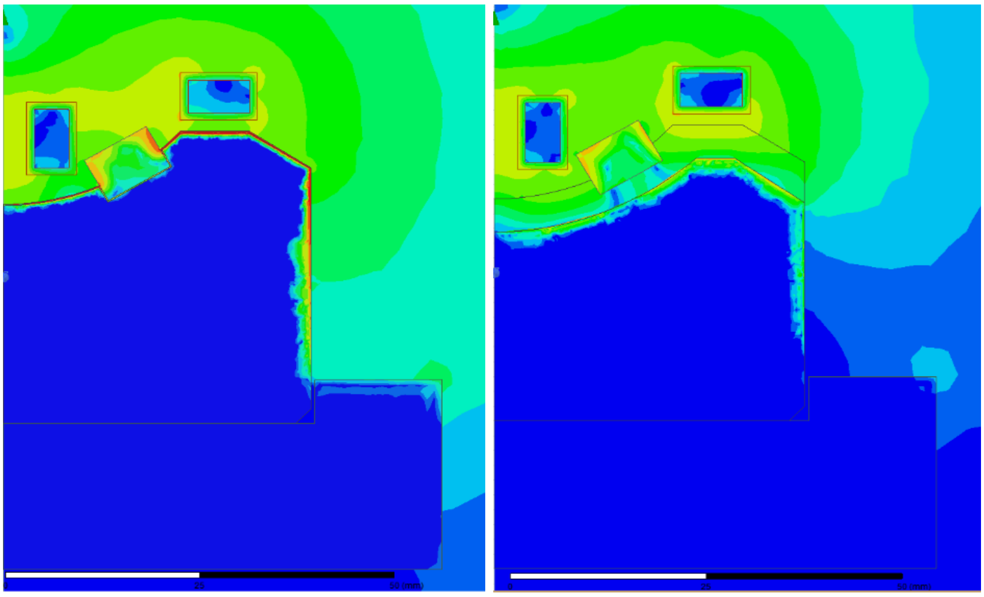

(a) **(b)**

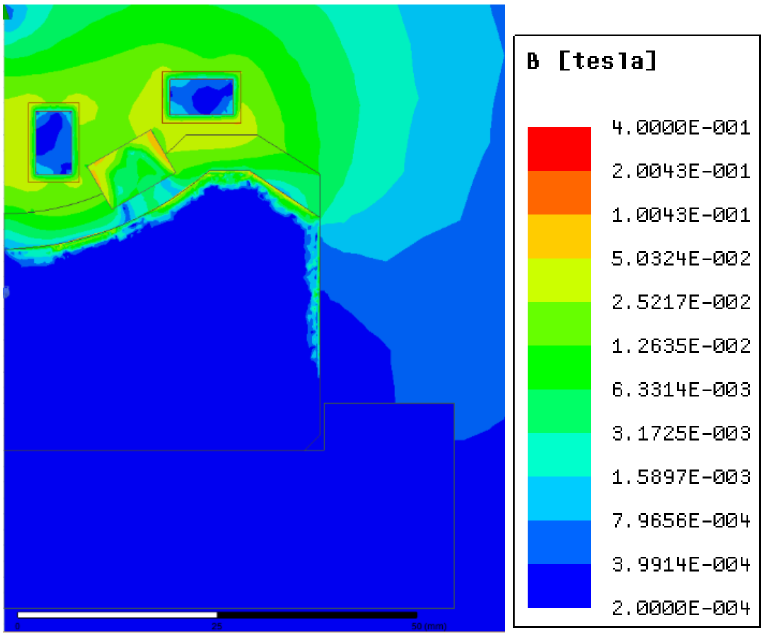

(c)

Fig. 25 – (a) Improved coil design with jaw at 25 °C, (b) Improved coil design with jaw at 770 °C, (c) Outer conductor shifted closer to the inserts with jaw at 770 °C

Fig. 25 (c) shows the effect of moving the outer conductor closer to the insert. It can be observed that the B-field is slightly more concentrated around the jaw and also penetrates the inserts more evenly. However, these gains are not sufficient to justify the movement of the outer conductor. This is because it is more beneficial to have a larger gap between the conductors, so as to ensure that the coil does not inhibit access for the insert retention mechanism discussed in Section 3.3.2. Therefore, the constructed coil shall follow the simulated geometry observed in Fig. 25 (b).

Construction of the physical coil involves cutting and bending sections of rectangular copper tube to the correct lengths. These sections can then be brazed together using an Oxy-Acetylene torch and silver solver. A silver solder or brazing alloy is better suited for use in high temperature applications such as that of induction coils than a standard Sn-Pb solder. This is because it has a higher melting point, thereby preventing meltdown of the coil joints due to radiant heat from a work-piece. The physical coil that was constructed as a result of the simulation work carried out can be observed in Fig. 26.

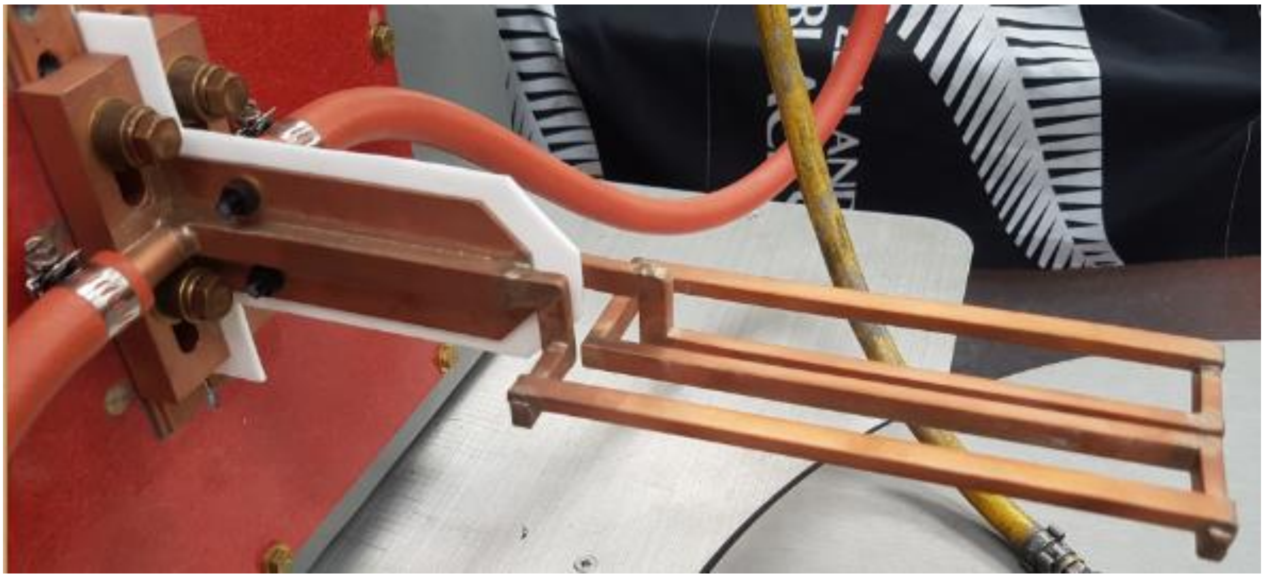

Fig. 26 – Constructed improved coil

3.3.2 Development of Insert Retention

Due to the high pressure abrasive nature of their use, the surface across all the inserts in jaws must be level. During initial brazing trials, it became apparent that the tungsten-carbide inserts become attracted to the coil when it is energized, resulting in the inserts jumping out of the slots and shorting the coil to the work-piece. This is because tungsten-carbide is a composite material containing paramagnetic and ferromagnetic materials as binders. The grade of tungsten-carbide in use is made up of 90% Tungsten, which is paramagnetic, and 10% binder materials including Cobalt, which is ferromagnetic. Thus, when exposed to the strong field generated by the induction coil, the inserts become attracted to the coil. To resolve this issue a method of retaining the inserts during the heating process must be developed alongside the improved coil, as any coils designed must allow room for the mechanism. Any insert retention technique must suit the shape of the jaws.

There are several types of jaws in production at Heat Treatments. Each type is used for gripping a different sized shaft and, therefore, has a differing radius and spacing between the milled slots. The three, high volume ‘8’ series jaws are all 120 mm long, by 80 mm wide, and have a maximum thickness of 40 mm. The spacing between the tungsten-carbide inserts, as specified in Fig. 27, varies from 20 mm to 37 mm, but the pitch of the inserts remains constant at a 30° angle. The ‘5’ series jaws are much larger, and more challenging to design a coil for. These will only be addressed in future work, due to the time constraints on this research.

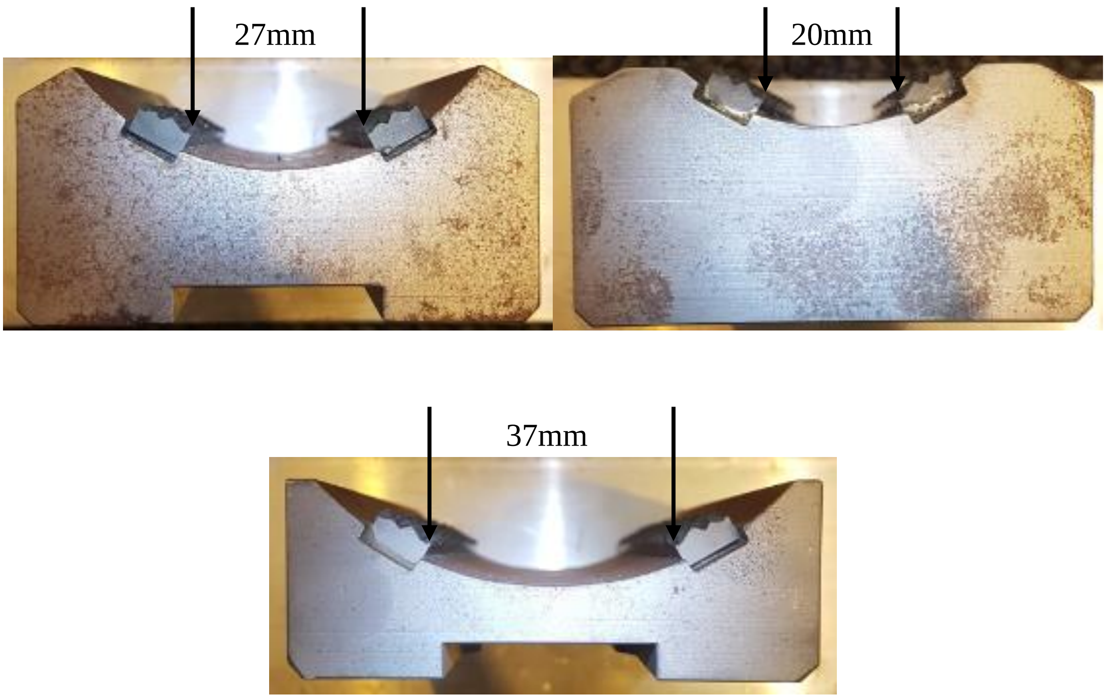

Fig. 27 – ‘8’ series jaws produced by Heat Treatments

Due to the differing pitch of the jaws, the developed mechanism must either be adjustable or able to service all jaw types. Thin, austenitic stainless-steel wires could be used to clamp the inserts down during brazing. However, the wire will expand too much as a result of the radiant surface heat from the jaw, causing it to bow. This may allow the center inserts to raise and become brazed in a slight arc. Thus, one of the key challenges surrounding the design is the high temperature nature of the brazing process. Fire brick could present a simple approach to the development of a suitable mechanism. It is soft enough to cut and shape with simple hand tools, reducing development time, and is sufficiently heat resistant. However, this material is significantly lighter than a ceramic, and therefore would require mounting on some rigid structure. This is not practical, as fire brick is brittle. The most practicable material for insert retention was identified as high temperature castable, or machinable, ceramic [46].

Fig. 28 (a) and (b) pictures a cast ceramic block designed to sit over the coil that relies on its mass and gravity to hold the inserts in place. This block has sufficiently large contact surfaces that it is able to service all of the ‘8’ series jaws.

(a) **(b)**

Fig. 28 – (a) Ceramic insert retention part, (b) Insert retention part positioned on a jaw

A test batch of 80 jaws were processed using the new ceramic block, of which, 60% required re-working, due to one or two inserts being incorrectly seated in the slots. In order to re-work jaws, extra pressure must be applied on top of the ceramic block when the jaw is heated to ensure correct seating of the inserts. Through examination of both the ceramic and jaws, it was found that brazing failure is due to slight misalignment of one or two inserts. Because the ceramic grips on the inserts, and because its load is spread, the inserts are effectively prevented from seating by the retainer. It is also noted that, occasionally, misalignment results from a buildup of flux residues on the contact faces. This suggests that a more robust method of insert retention would be to apply pressure on each insert individually. Doing so would minimize the opportunity for misalignment to occur and reduce the likelihood of flux buildups by reducing the area of ceramic in contact with the inserts. The mechanism designed must have a means of accurate adjustment, so as to service all of the ‘8’ series jaws. This will be discussed in future work.

Alongside coil design and insert retention development, work has been carried out on designing and implementing an automated loading mechanism for the induction heating machine. The jaws are required to be raised under the coil in a repeatable and accurate manner. It has been determined that the most reliable and efficient means of achieving the desired accuracy is to use either a partial, or fully automated loading mechanism. Therefore, a pneumatically actuated rotating table has been designed for the purpose of holding the assembled jaws and rotating them into position to be brazed. Once the jaw has been situated under the coil, a guided linear actuator lifts the jaw up into the desired position underneath the coil and insert retainer. After brazing, the jaw is lowered, and the rotating table indexed to move the next jaw into position. When the next cycle begins the operator will unload the hot jaw onto the cooling rack. The 3D model and the physically constructed system are pictured in Fig. 29 (a) and (b). At present, the system is only partially automated, thus the operator will manually actuate the rotating and lifting cylinders before and after the heating cycle. In addition to this, a timer circuit has been developed for the induction heater so as to ensure consistent heating cycles, and later enable the process to be fully automated.

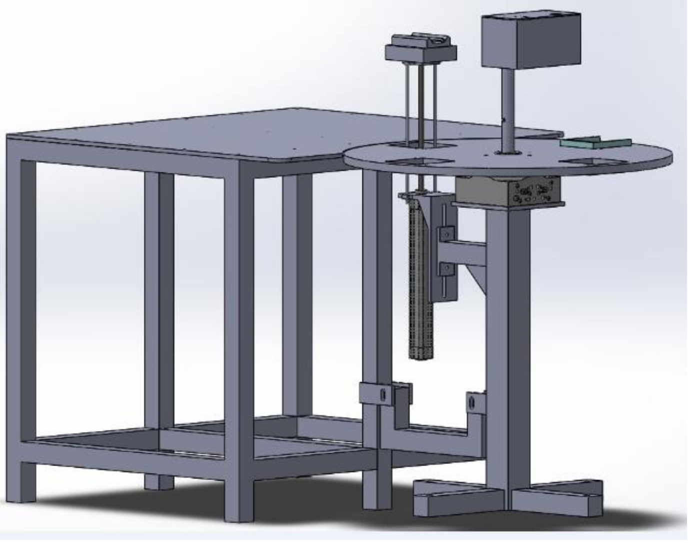

(a)

(b)

Fig. 29 – Semi-automated table design, (a) Solidworks model, (b) Physically constructed system

3.3.3 Testing and Observations

Testing of the newly developed coil should be carried out to verify the effectiveness of the design and simulation work. This requires that a method of insert retention be applied to the coil. Given that this is still a work in progress; the ceramic block method shall be employed. This may not result in perfect seating of the inserts, but it will at least enable brazing to occur, if the coil functions as predicted. The same power (30%) and frequency (10 kHz) settings shall be used as in all previous tests, as recommended by Radyne.

The heating pattern, roughly 10 seconds into the cycle, can be observed in Fig. 30. It can be seen that the coil sits directly above the jaw, as per the simulated geometry, and that the induced heat is also concentrated in the center of the jaw. The dark, expanding heat pattern closely follows the curvature of the jaw. This pattern is a result of both the less concentrated, expanding field's interaction with the jaw, and thermal conduction of surface heat. As time passes, the induced surface heat is drawn via thermal conduction throughout the steel, but not sufficiently to raise the whole jaw to brazing temperature.

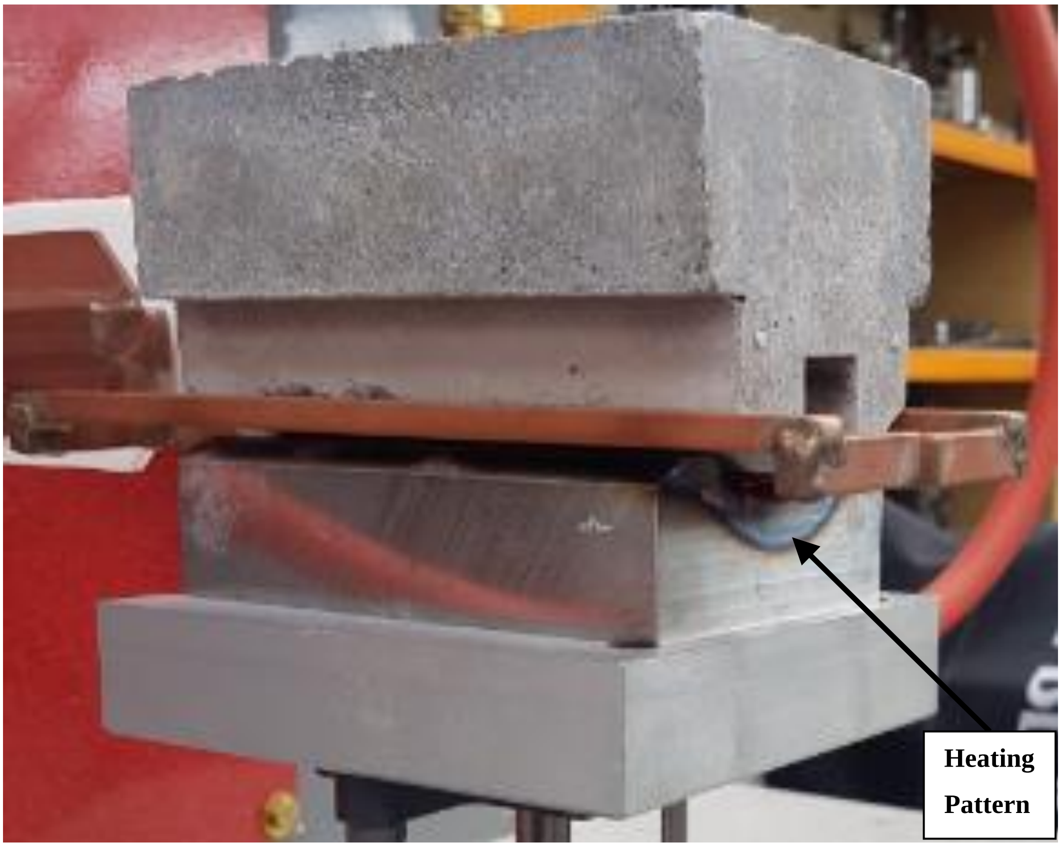

Fig. 30 – Testing of improved coil showing initial heating pattern

Therefore, as can be observed in Fig. 31 (a) and (b), roughly 35 seconds into the cycle, the darker pattern has spread over most of the jaw. However, it is clear that the field distribution is greatly improved over previous trials, with the majority of induced heating occurring in the desired region surrounding the slots and inserts. To further support this, the overall cycle time was able to be reduced from over 1 and a half minutes to just 45 seconds, with no scaling of the jaw surface. Comparison of this trial with the simulations observed in Fig. 25, (a) and (b), reveals that the induced heat pattern closely follows the field distributions predicted at both initial and final temperatures. The majority of heating occurs surrounding the slots and inserts as projected, whilst a small amount of induced heating occurs on the sides and ends of the jaw due to the stray field's interaction with the jaw. The result of this trial was not only a successful braze, but reduction of the cycle time by half, minimal oxidation and scaling of the jaw, and a relatively even heat distribution across the desired region.

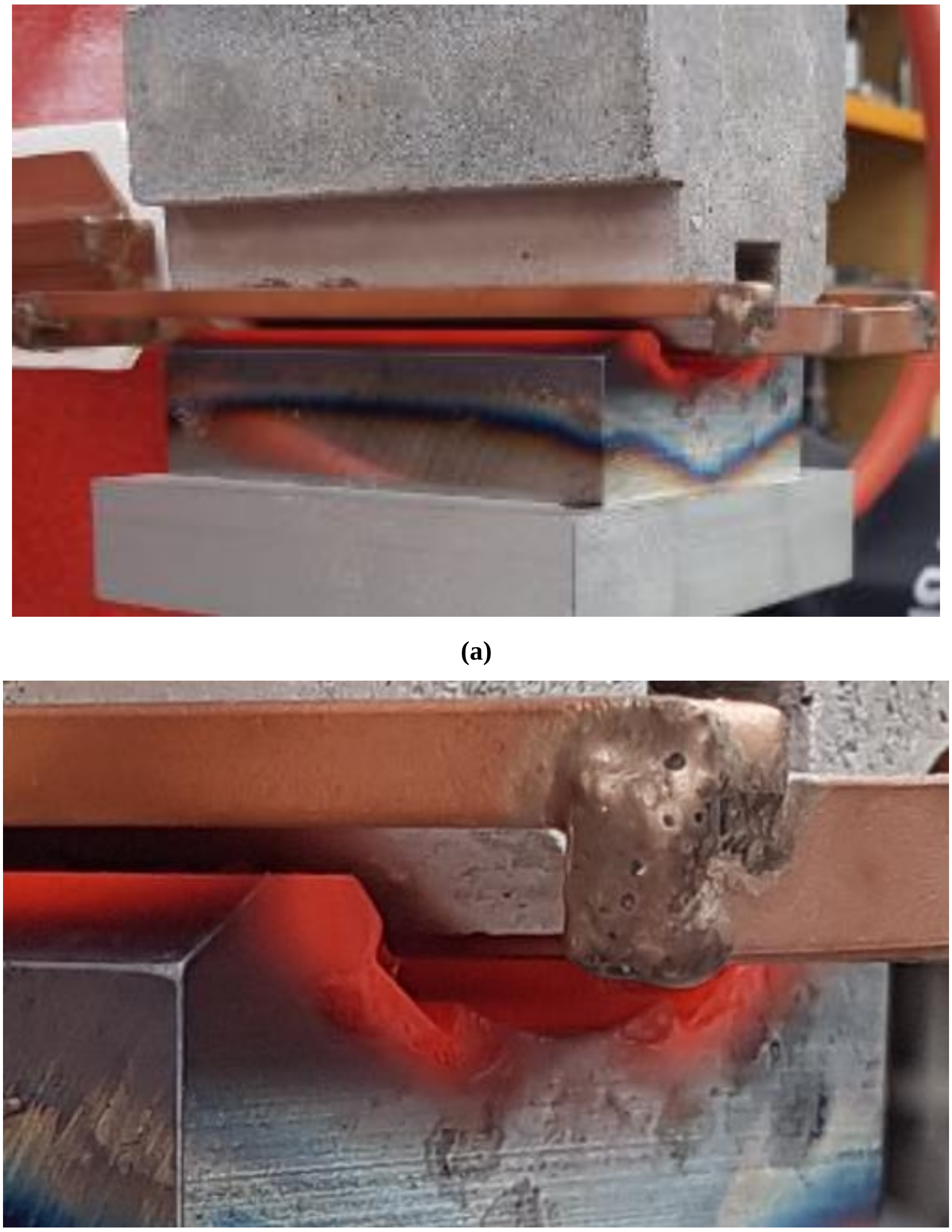

(a)

(b)

Fig. 31 – (a) Improved coil heating pattern near end of cycle (steel near Curie), (b) Close-up of heating pattern generated by the new coil

3.4 Summary

In this chapter, the issues of poor heating effect and insert retention were identified for the commercial induction brazing system. The FEM modelling work identified that an improved heating pattern would result from unidirectional current flow through the central conductors of the induction coil. Based on modelling an improved coil was designed and constructed. The outcome of the trial conducted was not only successful brazing, but a reduction of the cycle time, minimal oxidation and scaling of the jaw, and an even heat distribution across the desired region. This shows superior performance over that of the commercial system. The issue of insert retention was also discussed and a potential solution was proposed. Work carried out on the development of an automated loading mechanism and heat cycle timer was also briefly discussed.

In Section 3.2 and 3.3, it was identified that the operating frequency of the present power supply is not optimal for this application. The results of FEM modelling support this conclusion, as it was observed that the B-field present beneath the inserts is very low. In addition, it was identified that the field surrounding the coil is still un-concentrated. These shortcomings shall be investigated in Chapter 4.

Chapter 4

Design of an Optimal Coil and Operating Frequency

4.1 Introduction

The simulations and testing carried out in Chapter 3 suggest that the 10 kHz frequency of the power supply in use is not ideal for this application. This is clear through the lack of B-field penetration in the desired region beneath the inserts as observed in the FEM model. Additionally, the FEM model of the improved coil developed showed that the field is still significantly un-concentrated. Therefore, investigations into an optimal operating frequency and coil design that satisfies the design constraints have been undertaken and will be discussed in this chapter.

Section 4.2 documents and discusses the relevant material properties and the selection of the operational frequency that are to be applied to FEM models. Section 4.3.1 presents the design of the flux concentrator and induction coil to be implemented. The results of FEM modelling are then presented and discussed in Section 4.3.2.

4.2 Material Properties and Operating Frequency

The material properties, including relative permeability, of 1020 mild steel can be obtained with relative ease from various sources [42] [43]. However, material properties for tungsten-carbide are much more difficult to obtain. Therefore the properties used in simulations have been obtained from the manufacturer data sheets and direct communications (see Appendix B) [44], aside from relative permeability. For the purpose of approximating the relative permeability of the tungsten-carbide teeth used in this application, the following test was performed. A coil was wound around a small section of hollow plastic tube with 53 turns. The inductance of the coil was then measured using an LCR meter over a frequency range of 100 Hz to 10 kHz. One of the tungsten-carbide teeth can then be inserted inside the coil and a core constructed using three other teeth as seen in Fig. 32. It has been assumed that any air gap in the core has negligible effect on the measured values and, therefore, some error may exist. The measured values are given in Table 4.

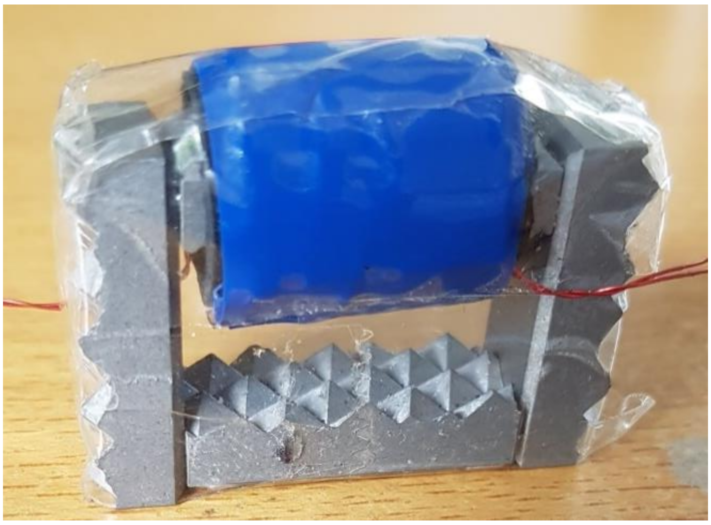

Fig. 32 – Measuring the inductance of tungsten-carbide for the calculation of permeability

Using these inductance values, the relative permeability can be approximated with knowledge of:

$$\mu = \mu_0 \mu_r = \frac{L \times l}{N^2 \times A} \tag{22}$$

It was thereby determined that the tungsten-carbide inserts in use have a relative permeability of approximately 12 at 10 kHz, as is used for the FEM models in Chapter 3.

Assuming a single frequency power supply is used, the frequency should be ideally set to provide a skin depth that penetrates through the tungsten-carbide and into the base of the slot to eliminate the shielding effect of the inserts. Fig. 33 (a) and (b) have been formed to display the frequency vs skin depth relationship for tungsten-carbide and 1020 mild steel at 25 °C and 770 °C. As can be observed, even at a low frequency of 500 Hz, penetration right through the inserts would not be achieved. It can also be seen that when the jaw reaches Curie temperature, the effective skin depth would be close to 20 mm in the 1020 mild steel, thus drawing a significantly larger amount of power from the supply. Operating at this frequency would be highly inefficient and, therefore, a compromise must be made. This highlights the absence of a single optimal frequency, as the variance of skin depth with temperature in each material due to their differing material properties cannot be accounted for in a single frequency. Therefore, an improved operating frequency is proposed instead. The higher the frequency, the lower the power required [2]. To achieve greatest efficiency, the chosen frequency must result in suitable field strength present beneath the inserts whilst minimizing power consumption. For this reason, a frequency of 4 kHz shall be trialled. This will result in a penetration depth of approximately 7 mm into the 1020 at Curie temperature, and approximately 2 mm in the inserts. Given the results of the previous simulations at 10 kHz, and the additional application of a flux concentrator, this frequency should provide sufficient field penetration beneath the inserts when at brazing temperature. At 4 kHz the relative permeability of the tungsten-carbide is determined to be approximately 14.

Table 5 contains the material properties that shall be used in all simulations and calculations in this Chapter.

Frequency (kHz)	**Without Tungsten-carbide (μH)**	**With Tungsten-carbide core (μH)**	**Relative Permeability, μ_r**
0.1	23.8	33.3	15.37
1	23.8	32.95	15.21
2	23.8	32.1	14.82
3	23.8	31.05	14.33
4	23.8	29.97	13.84
5	23.8	28.9	13.34
7.5	23.8	26.9	12.42
10	23.8	25.57	11.8

Table 4 – Inductance and relative permeability of tungsten-carbide core

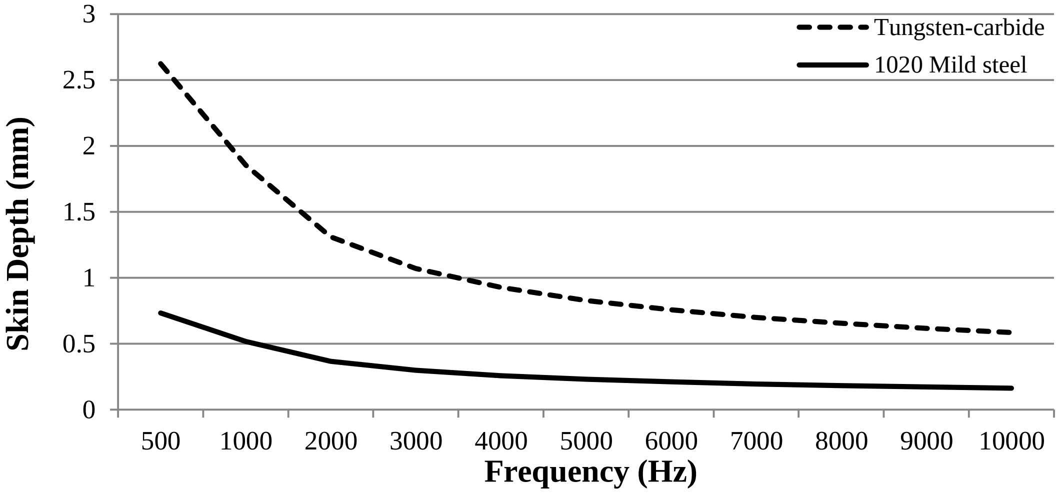

(a)

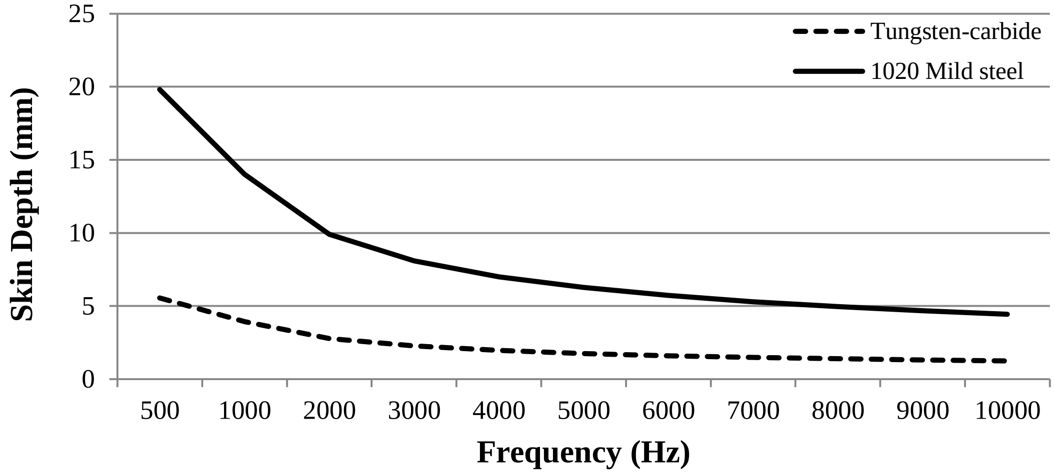

(b)

Fig. 33 – Skin Depth VS Frequency at, (a) room temperature (25 °C) and (b) Curie temperature (770 °C)

Table 5 – Material Properties – (see also Appendix B)

Properties	**Materials**	
	1020 Mild steel [42] [43]	***Tungsten-carbide – 10% impurity*** [44]
Resistivity (25°C)	0.159 μΩ/m	0.19 μΩ/m
Resistivity Temp. Coefficient	0.005	0.0045
Electrical Conductivity	$0.62893*10^7$ S/m	$0.526316*10^7$ S/m
Thermal Expansion	12 μm/m-K	6.5 μm/m-K
Density	$7.872*10^3$ kg/m^3	$15*10^3$ kg/m^3
Relative Permeability (25°C)	150 H/m (approx.)	14 H/m at 4 kHz (approx.)
Curie Temp.	770 °C	950 °C – 1050 °C [41]

The most suitable flux concentration method identified in the literature survey was that of ferrite pieces and MDM's. Due to the practicality of having a malleable material that does not require machining or adhesives for joining, the flux concentrator shall be implemented using Fluxtrol's Alphaform LF [37]. The only extra process involved with the use of this product is that it must be fired in a furnace once fitted to the coil, before use. It is during firing that it gains mechanical strength and loses its ductility. The relevant material properties of this product are listed in Table 6.

Table 6 – Properties of Fluxtrol Alphaform LF – (see also Appendix C)

Property	**Alphaform LF** [37]
Saturation Flux Density	1 T
Resistivity	> 15 kΩ cm
Maximum Permeability	13
Initial Permeability	11

4.3 Calculations and Simulations

4.3.1 Coil and Concentrator Design

Given that the regions of the 1020 mild steel required to be heated are those beneath the two rows of inserts, it can be deduced that the ideal coil would have a hair-pin shape and sit directly over the inserts. With the application of E or U shaped flux concentrators, it is practically possible to achieve a suitably targeted heating pattern for such a hair-pin coil to be implemented. This style of inductor and concentrator design has been applied in many surface hardening applications [2]. If an E shaped core were to be used, a new coil would be required for each type of jaw due to the differing slot spacing's. Therefore, the general contour of the concentrator to be applied shall be a U shape. This is because the use of two U shaped cores can provide greater flexibility, enabling the coil to be adjustable. However, the final form and alignment of the concentrator and, therefore, the field's interaction with the work-piece is unique and requires further investigation. Thus, FEM analyses of differing concentrator designs have been conducted.

FEM work undertaken presents results for three concentrators with differing dimensions simulated at 770 °C. The minimum thickness of the concentrator material is 5 mm for all simulations. In Fig. 34, a U-piece with only a 1 mm gap between its legs and the inserts has been modelled. It can be observed that there is significant leakage field passing directly through the air gap and insert between the legs. Fig. 35 (a) displays the results of placing a 2 mm gap between the legs of the core and the inserts. This shows a reduction in the magnitude of the leakage field and also the field strength within the concentrator. As can be observed in Fig. 35 (b), when the gap is increased to 3 mm, there is further reduction in the magnitude of the leakage field present in the air gap between the legs of the flux concentrator and the inserts. The wider spread of the leakage field's interaction with the 1020 mild steel suggests this shape will practically result in a greater portion of the 1020 mild steel being heated than that of Fig. 34 (a) and Fig. 35 (a).

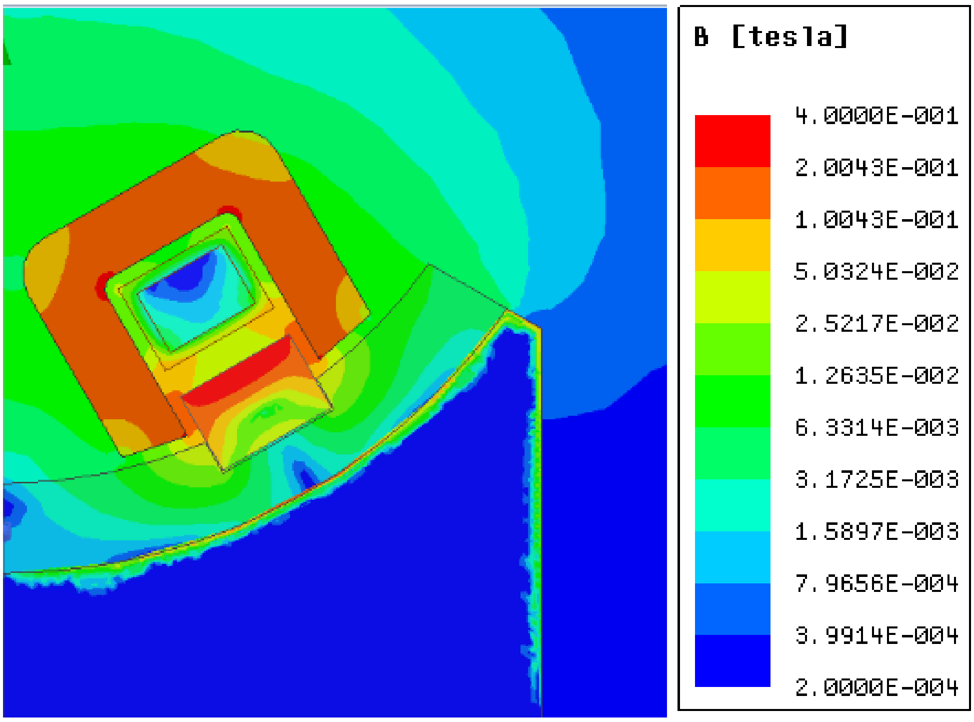

Fig. 34 – Flux concentrator with a 1 mm gap between insert and concentrator

These results can be confirmed through calculation also. By calculating the magnetic reluctance of the relevant paths, the effect of varying the size of the concentrator can be determined. This is due to the fact that as the reluctance of a path increases, the magnetic flux present in that path decreases. Therefore, Fig. 36 models the flux concentrator and coil position above the jaw and the parameters used for the calculations are established.

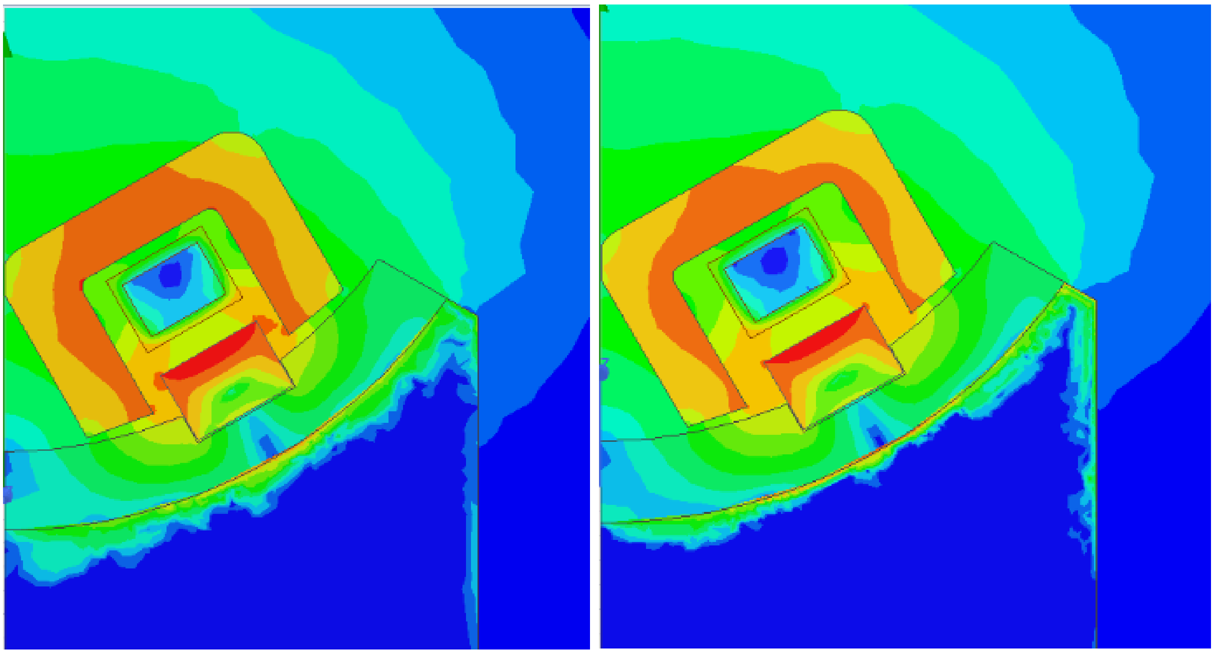

(a) **(b)**

Fig. 35 – Flux concentrator with, (a) 2 mm gap, (b) 3 mm gap

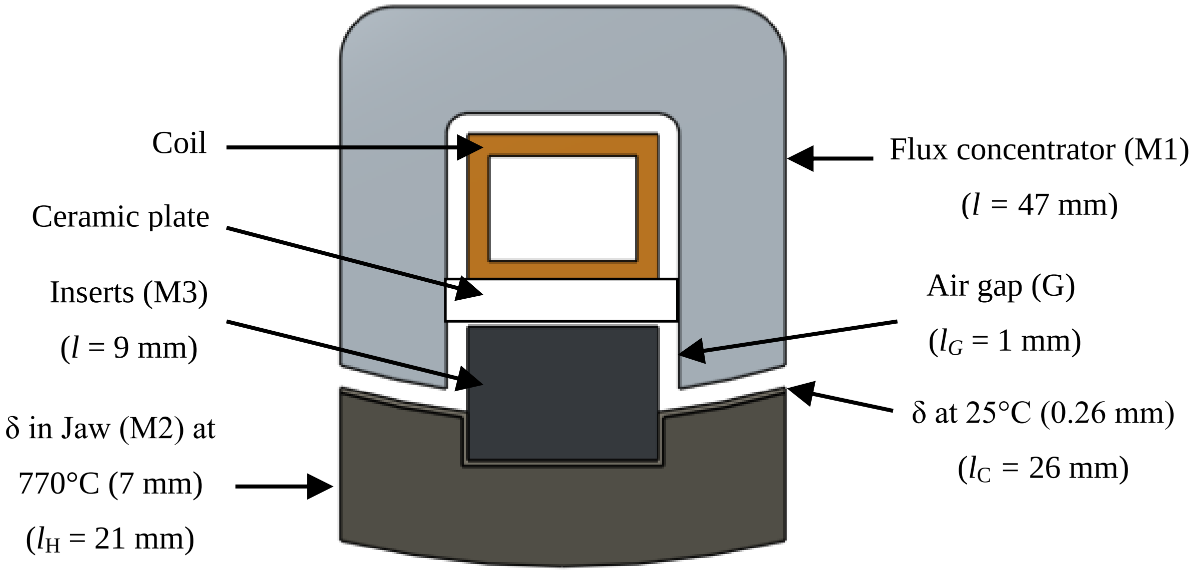

Fig. 36 – Flux concentrator positioned above skin depth portion of a jaw

Using equation (28), the reluctances of the path through the concentrator (M1) and the air-gap (G) have been calculated for the spacing's of 1 mm, 2 mm, and 3 mm between the inserts and the concentrator. The areas used in calculation for G and M1 are 0.0006 m^2 and 0.00072 m^2. The results have been tabulated in Table 7.

$$R = \frac{l}{\mu_0 \mu_r A} \tag{23}$$

Table 7 – Calculated Reluctances

Path length in G (m)	**Path length in M1 (m)**	**Reluctance of M1 (H^{-1})**	**Reluctance of G (H^{-1})**
0.001	0.047	4795052.773	1105242.66
0.002	0.0494	5039906.531	2210485.321
0.003	0.0504	5141928.931	3315727.981

It can be observed from these calculated values that whilst variance in the reluctance of M1 is minimal, the air gap reluctance increases by 100% of its initial value with every 1 mm increase in gap size. When these calculations are compared with the FEM models, it can be seen that there is agreement between both sets of results. In Fig. 35 (a) the magnitude of the field strength within the concentrator and the air gap are both reduced. However, with the air gap presenting a substantially lower reluctance than the concentrator, this reduction is more pronounced in the concentrator. When the gap is increased to 3 mm, there is further reduction in the magnitude of the field present between the inserts and the concentrator, as observed in Fig. 35 (b). It could therefore be said that further increasing the size of the air gap would result in improved field distribution. Closer observation of Fig. 35 (a) and (b) reveals that this assumption would be incorrect. It can be seen that the field strength beneath the inserts is greater in (a) and begins to dissipate in (b), with a small dark blue region visible. Thus, an optimum spacing could be determined.

Despite evidence that supports the increased air gap between the concentrator and inserts, this is practically not suitable for the application. This is due to the fact that spacing between the inserts varies between the three ‘8’ series jaws. Therefore, the gap between the conductors of the hair-pin coil must also be varied to suit. Consequentially, implementing a 3 mm gap is not possible, as the two concentrators will interfere if used on an adjustable coil. The only method of achieving this gap would be to form an E shaped core. The disadvantages of this have already been discussed and, therefore, this shall not be considered. Thus, the implemented design shall be one in which the air gap is kept to a minimum, such as that of Fig. 34. Further FEM analyses shall be carried out on this model.

4.3.2 FEM Modelling

A series of cross-sectional FEM models have been generated, accounting for the effects of temperature variation. Using the models, simulations have been performed to observe the effectiveness of coil configurations with magnetic field focusing and with coil currents of 800 A. As discussed in Section 4.2, operation at a lower frequency of 4 kHz allows for a skin depth of 7 mm in the 1020 mild steel jaw at the brazing temperature. This gives deeper magnetic field penetration. Further, with the introduction of a U-shaped core, the magnetic field can be guided to improve penetration at the bottom of the slot. Therefore, the results of modelling are presented based on a core implemented in Alphaform LF [37], fitted over the coil. The properties of Alphaform LF are given in Table 6 and for the FEM model, the relative permeability is set at 13. The core is shaped to conform closely with that portion of the insert proud of the slot. This is practically possible, as the core material is ductile, and can be shaped before being cured. To account for changes in magnetic diffusivity with temperature, simulations are presented with material properties set at 25 °C, 500 °C and 770 °C values. For each temperature the skin depth is changed in accordance with changes in magnetic diffusivity.

Fig. 37 models the jaw at 25 °C when the coil has just been energized. It is apparent that the field concentration is significantly improved over that of Fig. 25 (a). Fig. 38 (a) and (b) depict the B-field interaction with the jaw and inserts at 550 °C and 770 °C. It is apparent a significant leakage field exists between limbs of the u-shaped core as discussed in Section 4.3.1. However, it can be observed in both Fig. 37 and Fig. 38 (a) and (b), that the magnetic field present at the bottom of the slot is greater, at all temperatures, than those shown in Fig. 25 (a), (b), and (c). This shows superior performance. Therefore, it can be presumed that experimental testing of the coil with flux concentration will result in significantly reduced cycle times and increased electrical efficiency. This assumption is justified given that practical testing of the coil in Fig. 25, with lesser field penetration, resulted in successful brazing and improved efficiency. Furthermore, the field strength in Fig. 38 (a) and (b) is also much greater in the regions within and surrounding the inserts due to the presence of the flux concentrator. This suggests that the coil current may be able to be lowered whilst still achieving satisfactory field penetration beneath the inserts. To confirm this, simulations have been carried out with both 750 A and 500 A coil currents at Curie temperature, as depicted in Fig. 39 (a) and (b).

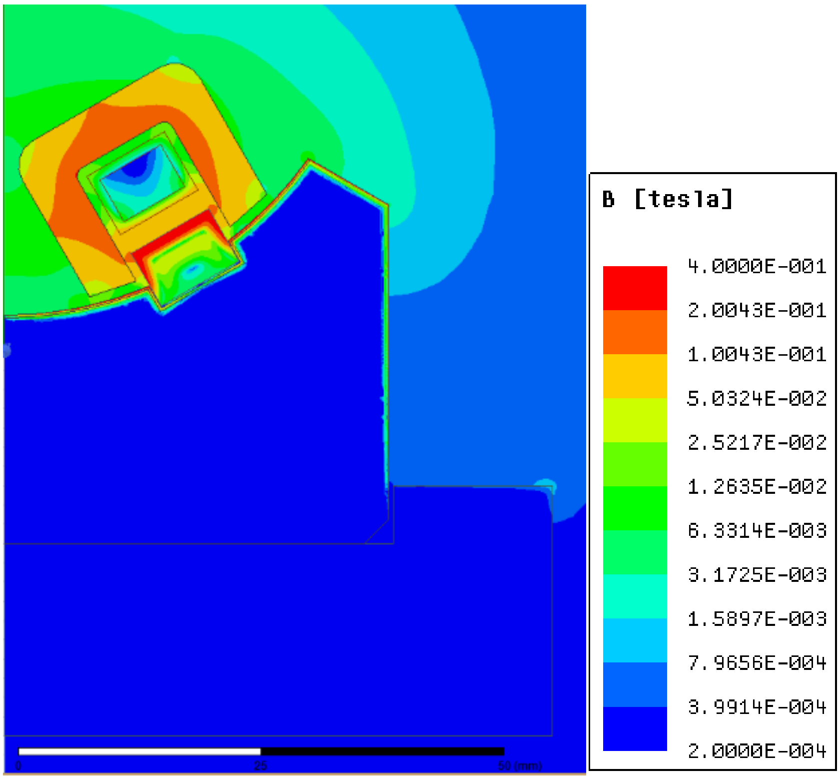

Fig. 37 – 2D model of coil and concentrator at 4 kHz and jaw at 25 °C

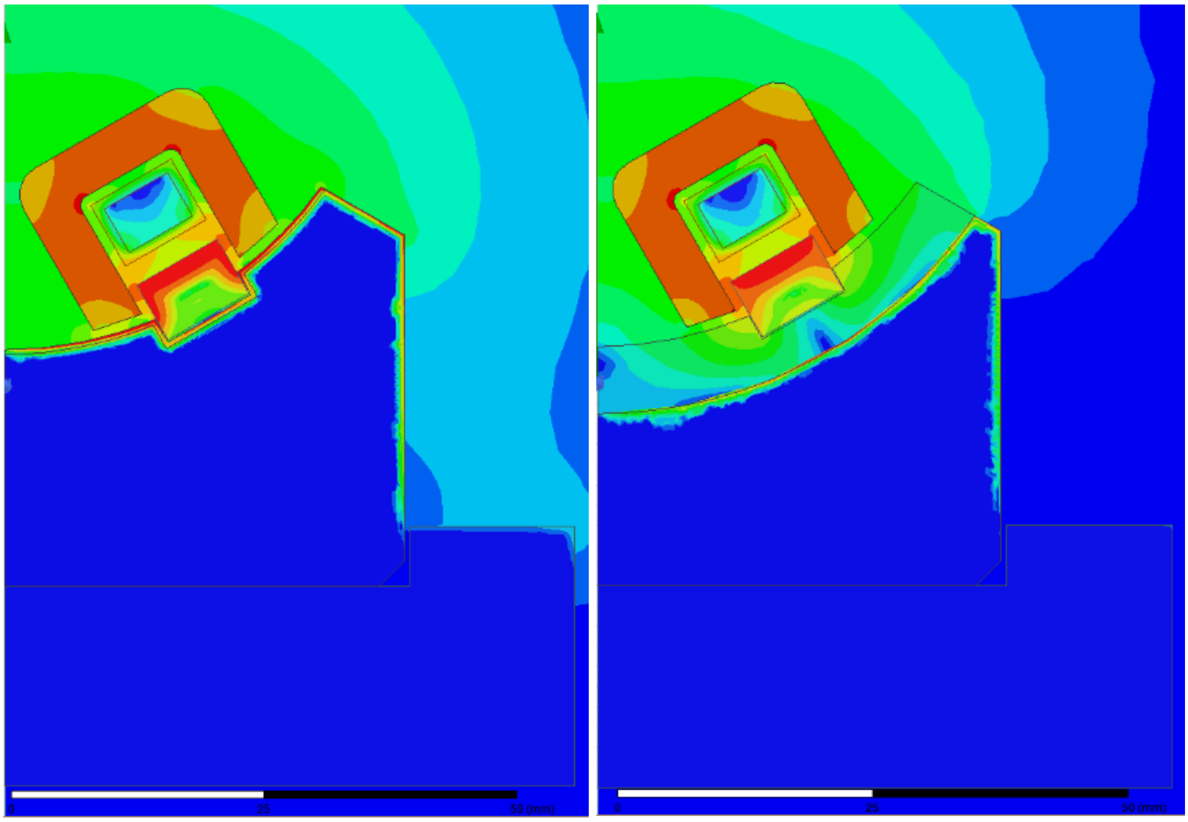

(a) **(b)**

Fig. 38 – Magnetic field with guidance at 4 kHz, (a) 550 °C, (b) 770 °C

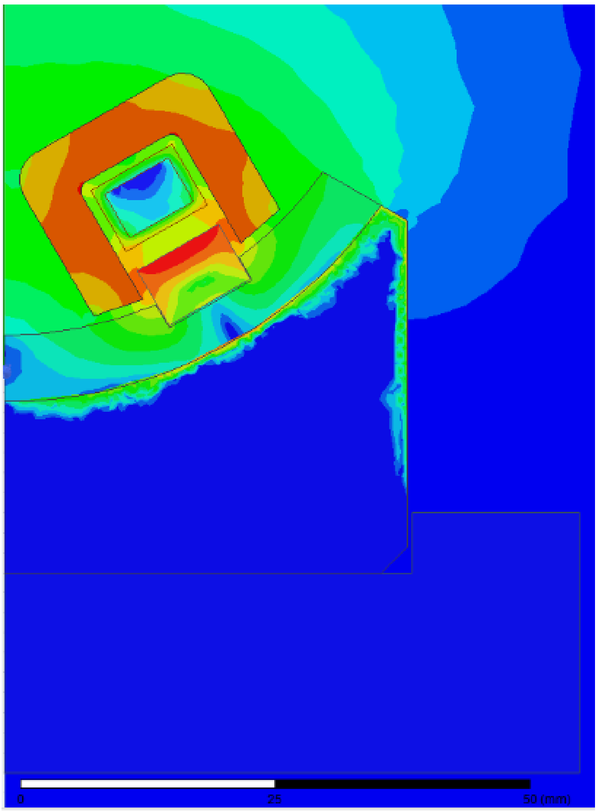

(a)

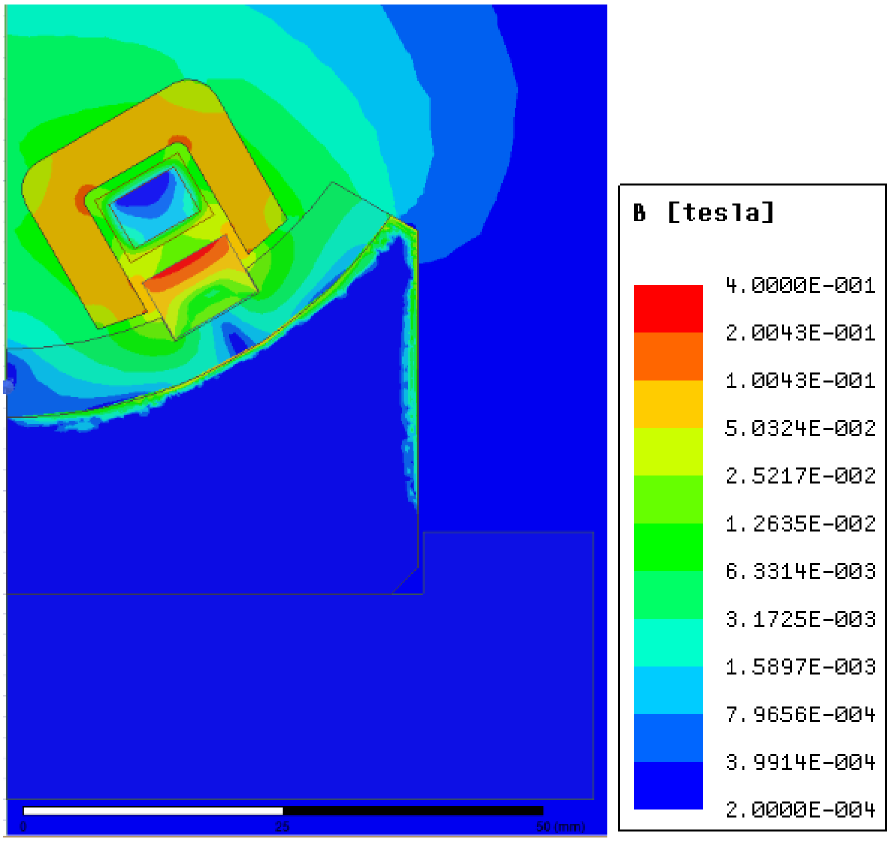

(b)

Fig. 39 – Magnetic field with guidance and jaw at 770 °C with, (a) 750 A coil currents, (b) 500 A coil currents

As can be observed from Fig. 39 (a) and (b), the addition of the flux concentrator has resulted in a significant improvement in electrical efficiency. This is confirmed by the fact that the field strength, within, beneath and surrounding the inserts, with a coil current of just 500 amps is on par with that observed in Fig. 25 (b). Also, the field in and surrounding the skin depth portion of the jaw is significantly more concentrated. This means that heating will be focused within a smaller portion of the jaw, therefore demanding less power. It can also be observed that the improved frequency of 4 kHz allows for greater penetration within and beneath the inserts. Given that the coil simulated in Fig. 25 has been experimentally validated, resulting in a successful braze, it can therefore be suggested that even with 500 A coil currents, similar brazing times will be achieved.

4.4 Summary

The results presented in Section 4.3 indicate operation at 4 kHz is an improvement over the existing system with poor magnetic field guidance operating at 10 kHz. Furthermore, the development of a U shaped flux concentrator and hair-pin coil resulted in significantly improved field concentration in the region in need of heating. Assumptions can be made that these theoretical models will hold true in practice, as for the coil development discussed in Chapter 3. When allowing for skin depth at 770 ^{o}C, a section of the 1020 mild steel material is assigned a permeability of 1 for a distance from the jaw surface equal to the skin depth. This is justified by the fact that 86.5 % of heating power is concentrated within one skin depth. However, this assumes thermal conduction does not allow for significant heat penetration beyond the skin depth, in a heating period. In practice, such a clear delineation between hot and cold parts of the jaw may not exist, as the drop in temperature from one skin depth to inner parts of the jaw may be more gradual. In turn, this would lead to a more gradual change in skin depth. The trials carried out using the Radyne coil (Fig. 19) show that there are visible hot and cold areas on the surface of the jaw. However, due to the lack of concentration, induced heating occurs on all surfaces, to a limited extent, making it difficult to accurately observe the effect (if any exists) of thermal conduction during the heating cycle.

The results of the FEM models presented in this chapter suggest the proposed coil can achieve significantly improved performance compared to the commercial system and the improved coil developed in Chapter 3. It is thought however, that this coil and operating frequency will still result in some reliance upon thermal conduction. The 7 mm penetration depth can only be achieved after the initial skin depth portion of 1020 mild steel reaches Curie temperature, thus allowing the skin depth to increase and repeat this pattern. Due to the fact that this process is not instantaneous, thermal conduction will occur.

Having confirmed the need for a lower operating frequency of 4 kHz, the future work section of Chapter 5 shall briefly discuss the development of a suitable power supply. Future work includes experimental verification of the modelling work.

Chapter 5

Conclusion and Suggestions for Future Work

5.1 General Conclusions

The design of a magnetic component for induction brazing of tungsten-carbide inserts into 1020 mild steel, where all surfaces of the brazing region are shielded, has been investigated in this Thesis. As a result of initial investigations, several constraints were identified including; material properties, operational frequency, and the requirement of insert retention for successful brazing. A partial solution neglecting the use of a flux concentration material was modelled and validated through practical experimentation, resulting in improved performance. The shortcomings of this partial solution were identified and a new model proposed implementing a magnetic flux concentrator and improved frequency. Modelling results for the full solution show significant field penetration resulted in the desired brazing region.

In Chapter 1 the commercial significance of the application was introduced. Issues with presently adopted vacuum brazing process were briefly explained, validating the investigation of induction brazing as a suitable alternative. The challenges posed by the application including the shielded nature of the brazing region were briefly addressed and reference to literature was made, identifying the contribution of this research to the induction brazing field of knowledge.

In Chapter 2 a literature review of previous work in the fields of induction brazing and magnetic field concentration was presented. The methods of electromagnetic field concentration were presented and evaluated with respect to their appropriateness for use in this investigation. Key considerations for successful induction brazing process design were discussed. To the best of the author’s knowledge, only one other application has been documented in which all faces of the region to be brazed via induction are shielded. However, in the author's opinion, the approach applied is inefficient. This shortcoming was addressed in Chapters 3 and 4.

In Chapter 3 critical analysis of a commercial induction heating solution provided by Radyne was undertaken. The issues of poor heating effect, ineffective coil design, and insert retention were identified and discussed. A solution proposed and implemented for the retention of tungsten-carbide inserts lead to inconsistent brazing. Therefore an improved solution was proposed in which pressure is applied to each of the inserts individually. The completion of this mechanism is referred to in future work. The issue of poor heating was addressed by means of FEM modelling and experimental validation. A coil with unidirectional current flow in its central conductors, and vertically off-set outer conductors was developed. Analysis of the heating pattern generated on the work-piece during practical testing of the developed coil closely followed the field distributions modelled using the FEM. Whilst improved performance and successful brazing resulted, observation was made that the field was not suitably concentrated and that the operational frequency is not optimal, as the B-field penetration in the desired region beneath the inserts in the simulated model was very low. This issue was addressed in Chapter 4.

In Chapter 4 investigations into an optimal frequency and concentrated coil design that satisfy the design constraints were presented through FEM modelling. It was identified through numerical analyses that the solution of a single optimal frequency (in its truest sense) for the application cannot practically be attained due to the differing effect of the frequency and temperature on the dissimilar materials. Therefore, an improved frequency is instead proposed. Additionally the design of an improved coil with suitable electromagnetic field concentration applied was documented. An analysis of FEM modelling results for when the spacing between the concentrator and inserts is varied was performed so as to identify the effect on the leakage field. It was determined that increased spacing would provide better performance, however due to the physical constraints presented by the spacing between the two rows of inserts, tight spacing shall be kept. The results of the FEM model for the proposed solution demonstrate a substantial improvement over the other coil designs discussed. Additionally the improved frequency results in greater penetration beneath the inserts at all temperatures, than that observed without a magnetic flux concentrator. Given that the lower 4 kHz frequency results in improved performance, the construction of a suitable power supply shall be discussed in future work.

To conclude, the research conducted has presented a method for the targeted induction brazing of tungsten-carbide into 1020 mild steel. The results of FEM modelling have suggested that this provides substantial improvements in electrical and heating efficiency. Further, the magnetic field penetration beneath the inserts has been greatly improved due to the selection of an improved operating frequency.

5.2 Contributions

The main contributions of this study are listed below:

- A solution that applies a focussed magnetic field to a brazing region that is surrounded on all sides by materials of differing properties has not been previously reported. This research proposes the use of a U shaped concentrator formed out of Alphaform LF
- Values are provided for the relative permeability of tungsten-carbide at several frequencies

5.3 Future Work

This section discusses the work still to be completed.

5.3.1 Continuing work from Chapter 3

Design work has been carried out on a possible solution to the insert retention problem. Fig. 40 depicts the current design developed on a software package called OnShape. In this proposed solution, the jaws will be lifted up to the ceramic fingers, which have only a small range of movement. The ceramic fingers have rubber stoppers under their end which act as cushioning, so as to avoid a hard stop, resulting in their breakage. Each finger is cast, and then the tip is precision ground to a 30 degree angle as required. Accurate Y-axis (as denoted in Fig. 40) adjustment will be provided by means of a sliding rail and ball-screw type mechanism, which has yet to be added to the drawing. These will be the only magnetic steel parts of the assembly, as they are far enough away from the coil. Vertical Z-axis adjustment has been accommodated for in the laser cut, slotted brackets that hold the ceramic fingers. Finally, X-axis adjustment has also been allowed for via slots as indicated. All parts of the assembly, besides the fingers and the Y-axis sliding rail, will be made of austenitic stainless steel (316). After installation and set up any further adjustment, should it be required, will be carried out by either adjusting the coil mounting position, or the pneumatic cylinder used for lifting the jaws up to the coil.

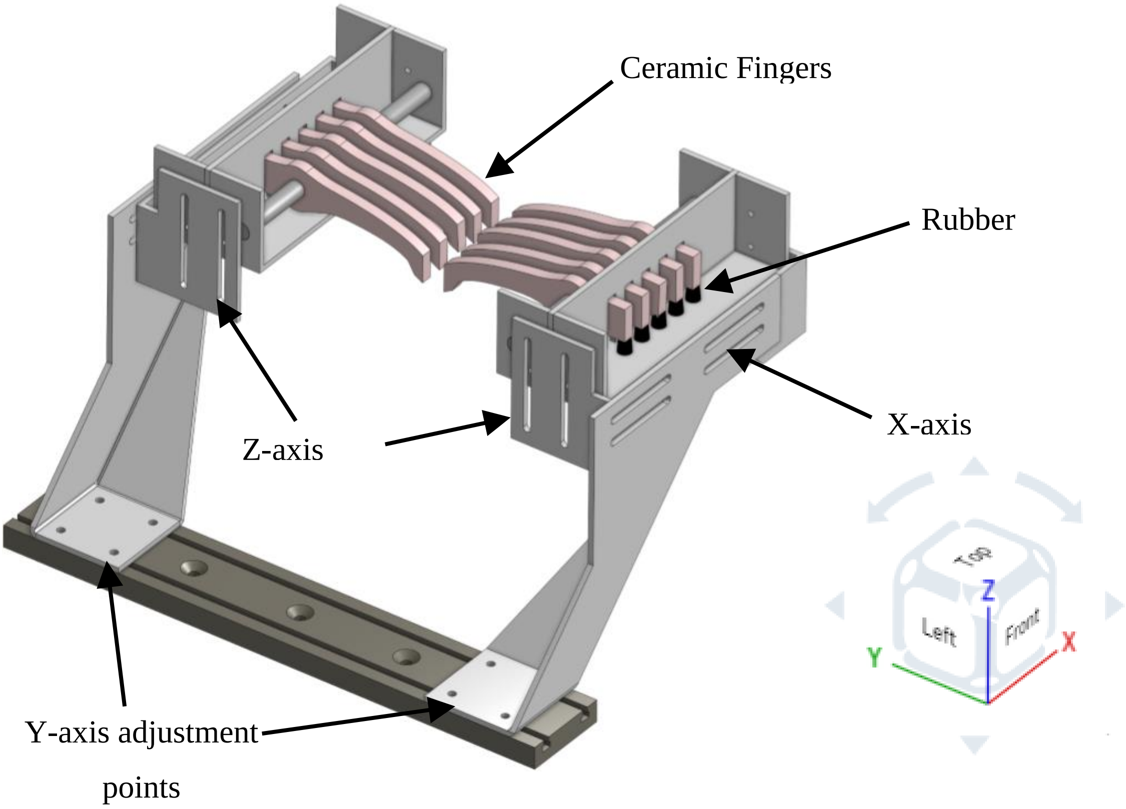

Fig. 40 – Insert retention mechanism

The next step is to physically construct the system and carry out a trial braze. Before this is carried out, the suitability of the ceramic material currently in use must be tested. Thus, a mold has been machined out of Aluminium, as depicted in Fig. 41, and a test finger has been cast and fired to 1000 °C. It was found that the ceramic has good strength and wear resistance properties making it well suited for this application. Construction shall be completed at a later date.

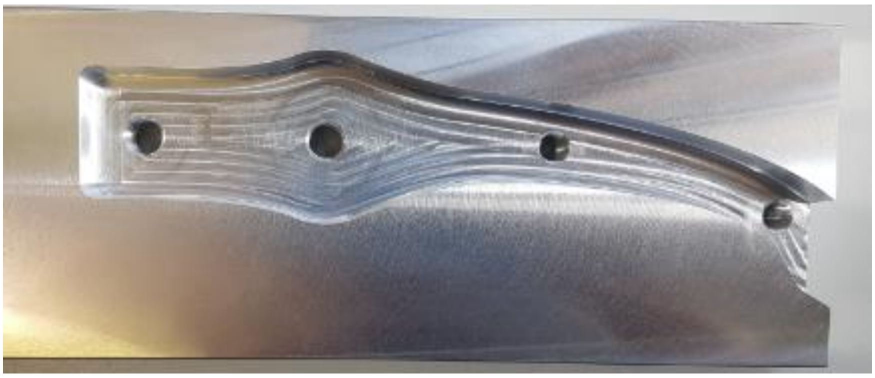

Fig. 41 – Mould for ceramic finger

5.3.2 *Continuing work from Chapter 4*

The results of the FEM modelling carried out in Chapter 4 confirmed the use of the improved 4 kHz frequency. Therefore, design work has been carried out and the construction of a suitable power supply capable of supplying 30 kW at a 4 kHz supply frequency has begun. The designed power supply and transformer can be observed in Fig. 42.

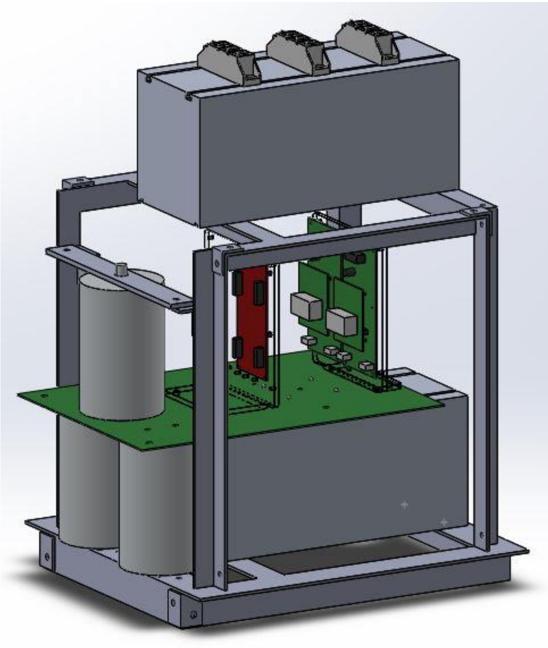

(a) **(b)**

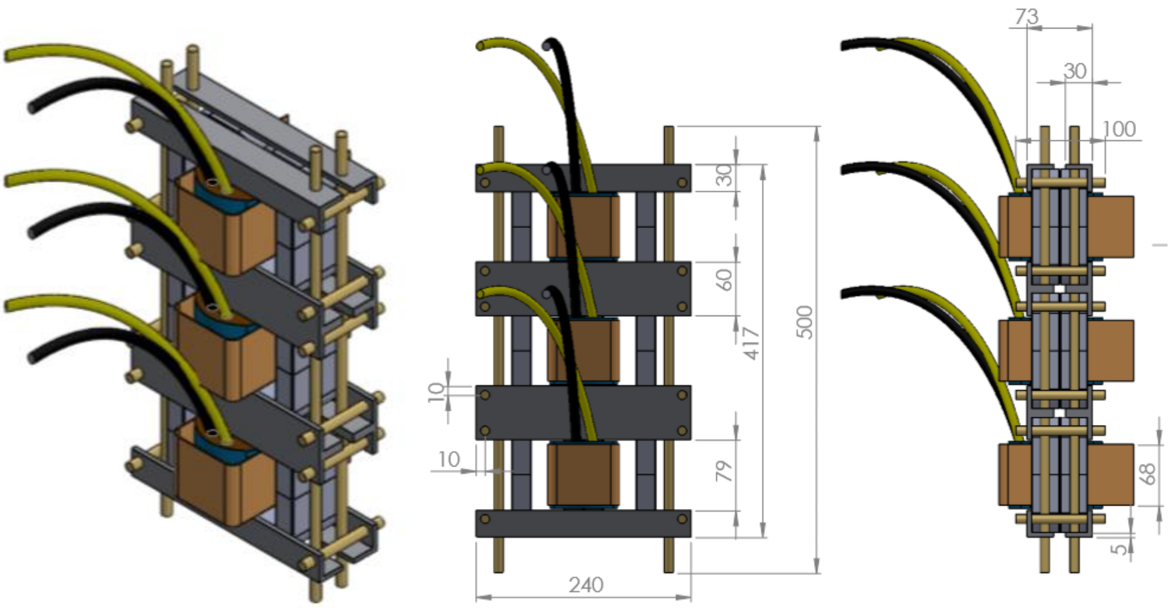

(c)

Fig. 42 - a) Solid Works drawing of supply, b) Progress on physical construction, (c) Transformer design

6 References

[1] Heat Treatments Ltd, [Online]. Available: http://www.heat-treat.co.nz/.

[2] V. S. Nemkov and R. C. Goldstein, Design Principles for Induction Heating and Hardening, Auburn Hills, Michigan, U.S.A.: Centre for Induction Technology, Inc., 2004.

[3] AMERITHERM INC, "How Induction Carbide Tipping Works: Ambrell," [Online]. Available: https://www.ambrell.com.

[4] M. H. Khazaal, I. M. Abdulbaqi and R. H. Thejel, "Modeling, design and analysis of an induction heating coil for brazing process using FEM," in *Al-Sadeq International Conference on Multidisciplinary in IT and Communication Science and Applications (AIC-MITCSA)*, Baghdad, 2016.

[5] D. N. Grozdanov and N. L. Hinov, "Industrial application of induction brazing systems," in *XXV International Scientific Conference Electronics (ET)*, Sozopol, 2016.

[6] H. E. Knoepfel, in *MAGNETIC FIELDS A Comprehensive Theoretical Treatise for Practical Use*, JOHN WILEY & SONS, INC., 2000, p. 258.

[7] S. Errede, "EM Fields & Sources," Illinois, 2007.

[8] D. L. V.I. Rudnev, "Induction Hardening: Technology, Process Design, and Computer Modeling," *ScienceDirect*, pp. 489-580, 2014.

[9] S. L. Semiatin, S. Zinn, I. L. Harry and R. D. Jeffress., Elements of induction heating: design, control, and applications., ASM International., 1988.

[10] P. M. Roberts, Industrial Brazing Practice, Chapman and Hall/CRC, 2013.

[11] Y. Wang, X. Yang, Y. Sun and L. Pang, "A New Inductor for Transverse Flux Induction Heating," in *Sixth International Conference on Electromagnetic Field Problems and Applications*, Dalian, Liaoning, 2012.

[12] V. K. Nisha, S. K and R. Acharya, "Modeling and simulation of multi coil induction heating system for semiconductor wafer processing," in *2016 IEEE International Conference on Recent Trends in Electronics, Information & Communication Technology (RTEICT)*, Bangalore, 2016.

[13] V. C. Valchev, T. P. Todorova, D. D. Yudov and D. J. Mareva, "Design considerations of inductors for induction heating of fluids," *19th International Symposium on Electrical Apparatus and Technologies (SIELA),* pp. pp. 1-3, 2016.

[14] Scott D. Sudhoff, "Magnetics and Magnetic Equivalent Circuits," in *Power Magnetic Devices: A Multi-Objective Design Approach*, 2014.

[15] J. M. Burdio, F. Villuendas, C. Carretero, J. Acero and J. M. Burdio, "Power losses in flux concentrators of inductor systems for induction cooktops," in *IECON 2017 - 43rd Annual Conference of the IEEE Industrial Electronics Society*, Beijing, 2017.

[16] H. T. Bui and S. J. Hwang, "Modeling a working coil coupled with magnetic flux concentrators for barrel induction heating in an injection molding machine," *International Journal of Heat and Mass Transfer,* pp. Pages 16-30, 2015.

[17] A. Lin, B. Pearce, C. A. Baguley, A. Findlay, M. Findlay and M. Causley, "The Design of a magnetic component to concentrate magnetic fields for localized induction heating," in *Proc. IEEE 2nd Annual Southern Power Electronics Conference (SPEC)*, Auckland, 2016.

[18] D. S. Kim, J. Y. So and D. k. Kim, "Study on Heating Performance Improvement of Practical Induction Heating Rice Cooker With Magnetic Flux Concentrator," *IEEE Transactions on Applied Superconductivity,* vol. 26, no. no.4, pp. pp. 1-4, June 2016.

[19] T. Zhu, P. Feng, X. Li, F. Li and Y. Rong, "The Study of the Effect of Magnetic Flux Concentrator to the Induction Heating System Using Coupled Electromagnetic-Thermal Simulation Model," in *International Conference on Mechanical and Automation Engineering,* Jiujang, 2013.

[20] P. Sergeant, U. Adriano, L. Dupre, O. Bottauscio, M. D. Wulf, M. Zucca and J. Melkebeek, "Passive and active electromagnetic shielding of induction heaters," *IEEE Transactions on Magnetics,* pp. vol. 40, no. 2, pp. 675-678, 2004.

[21] R. Bosshard, U. Iruretagoyena and J. W. Kolar, "Comprehensive Evaluation of Rectangular and Double-D Coil Geometry for 50 kW/85 kHz IPT System," *IEEE Journal of Emerging and Selected Topics in Power Electronics,* vol. 4, no. no. 4, pp. pp. 1406-1415, December 2016.

[22] I. Balabozov, H. Brauer and I. Yatchev, "Modelling of magnetic concentrators in induction heating systems," in *15th International Conference on Electrical Machines, Drives and Power Systems (ELMA)*, Sofia, 2017.

[23] P. L. Sergeant, L. R. Dupre, M. D. Wulf and J. A. A. Melkebeek, "Optimizing active and passive magnetic shields in induction heating by a genetic algorithm," *IEEE Transactions on Magnetics,* pp. vol. 39, no. 6, pp. 3486-3496, 2003.

[24] C. T. Rim and C. Mi, Wireless Power Transfer for Electric Vehicles and Mobile Devices, John Wiley & Sons Ltd, 2017.

[25] M. Chen, W. Liu, Y. Xi, C. Lin and S. Liu, "Localized induction heating for wafer level packaging," in *International Conference on Electronic Packaging Technology & High Density Packaging*, Beijing, 2009.

[26] D. P. Branko, P. M and P. Z, "Chapter 4 - Electromagnetic Induction," in *Fundamentals of Engineering Electromagnetics*, Taylor & Francis Group, 2006, pp. 123-162.

[27] F. Dughiero, M. Forzan and S. Lupi, "Solution of coupled electromagnetic and thermal problems in induction heating applications," in *Third International Conference on Computation in Electromagnetics*, Bath, 1996.

[28] J. Nerg and J. Partanen, "Numerical solution of 2D and 3D induction heating problems with nonlinear material properties taken into account," *IEEE Transactions on Magnetics,* vol. 36, no. no.5, pp. pp. 3119-3121, September 2000.

[29] M. C. Song and Y. H. Moon, "Coupled electromagnetic and thermal analysis of induction heating for the forging of marine crankshafts," *Applied Thermal Engineering,* pp. 98-109, 2016.

[30] L. Jakubovičová, A. Gašparec, P. Kopas and M. Sága, "Optimization of the Induction Heating Process in Order to Achieve Uniform Surface Temperature," in *Machine Modeling and Simulations*, Zilina, Slovakia, 2016.

[31] H. L. a. J. Rao, "Coupled Modeling of Electromagnetic-Thermal Problem in Induction Heating Process Considering Material Properties," in *International Conference on Information Engineering and Computer Science,* Wuhan, 2009.

[32] D. N. J. L. a. A. R. P. Masson, "Magnetic field concentration: comparison between several shapes of superconducting shields," *IEEE Transactions on Applied Superconductivity,* vol. 11, no. no. 1, pp. pp. 2248-2251, March 2001.

[33] S. Wenquan, Time-Domain Computer Analysis of Nonlinear Hybrid Systems, CRC Press, 2002.

[34] MEYER Tool and MFG. INC., "Selecting a Braze Filler Metal," [Online]. Available:

https://www.mtm-inc.com/av-20140130-selecting-a-braze-filler-metal.html.

[35] I. Piroi, E. Spunei, C. P. Chioncel, E. Raduca and F. Piroi, "Controlling the Variable Frequency Induction Heating," in *National Electric Driving Conference*, Cluj-Napoca, 2016.

[36] freebie.photography, "StockArch," [Online]. Available: https://stockarch.com/images/objects/metal-circular-saw-blade-teeth-9723.

[37] FLUXTROL, " Alphaform LF," [Online]. Available: https://fluxtrol.com/alphaform-LF.

[38] E. Dennison, "Off-Axis Field Due to a Current Loop," 2005. [Online]. Available: https://tiggerntatie.github.io/emagnet/offaxis/iloopoffaxis.htm.

[39] Radyne, "Radyne," [Online]. Available: https://radyne.com/.

[40] V. Rudnev, D. Loveless and R. L. Cook, Handbook of Induction Heating, CRC Press, 2017.

[41] A. a. C. Carbide, "All about Cemented Carbide," [Online]. Available: http://www.allaboutcementedcarbide.com/what-is-cemented-carbide/electrical-and-magnetic-properties/.

[42] SubsTech, "Carbon steel SAE 1020," 2012. [Online]. Available: http://www.substech.com/dokuwiki/doku.php?id=carbon_steel_sae_1020.

[43] MakeItFrom.com, "Cold Drawn 1020 Carbon Steel," [Online]. Available: https://www.makeitfrom.com/material-properties/Cold-Drawn-1020-Carbon-Steel.

[44] elementsix, *Abrasives - Cemented Carbide Grade K40L,* elementsix.

[45] F. W. Curtis, "High Frequency Induction Heating," in *High Frequency Induction Heating*, McGraw-Hill, 1950.

[46] Certec, "Certec," [Online]. Available: https://www.certec.co.nz/.

Appendix A:

AMERITHERM INC. Precision Induction Heating

AN AMBRELL COMPANY

Brazing carbide insert to steel pipe gripper chuck

Objective	To braze carbide inserts into steel blocks in the assembly of pipe gripper chuck
Material	Steel blocks,1" (25.0mm) wide X 3.5" (87mm) long and 2" (50mm) tall, toothed carbide inserts
Temperature	1450 ºF (780 ºC)
Frequency	192 kHz
Equipment	• Ambrell EASYHEAT 4.2 kW 400kHz induction heating system, equipped with a remote workhead containing one 1.0μF capacitor • An induction heating coil designed and developed specifically for this application.
Process	Blocks are fluxed and braze shims are sandwiched between the toothed carbide inserts and wells in the steel. A two-turn helical coil is used to heat the assembled part. A two-step heat profile flows the braze within 150 seconds per part
Narrative	Induction heating is proposed to replace a hand/flame process, delivering significant reduction in per-part cycles.
Results/Benefits	Induction heating provides: • Direct heating of the part, saving energy • Flameless process; doesn't 'blow' the braze • Precise control of heat • Process precision and repeatability for consistent results • Easy integrated into automated process • Even distribution of heating • Reduced flame hazard

Ambrell Companies

Ameritherm	Cheltenham Induction Heating	Ambrell	Ambrell
www.ameritherm.com	www.cihinduction.com	fr.ambrell.com	www.ambrell.com
+1.585.889.9000	+44 (0)1242 514042	+33 (0)3 89 76 01 24	+31 (0)548 659044

AMERITHERM INC. Precision Induction Heating

AN AMBRELL COMPANY

Testing configuration for feasibility

Block before braze (l), flame-processed (r)

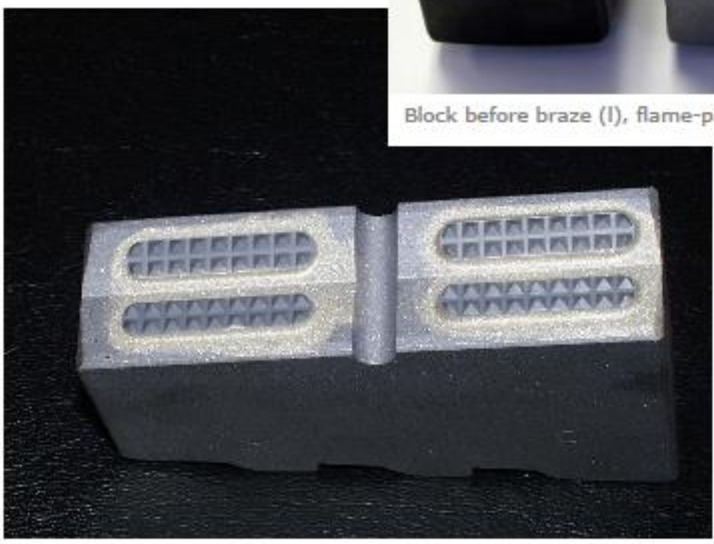

Finished gripper block with clean, uniform braze

Ambrell Companies

Ameritherm	Cheltenham Induction Heating	Ambrell	Ambrell
www.ameritherm.com	www.cihinduction.com	fr.ambrell.com	www.ambrell.com
+1.585.889.9000	+44 (0)1242 514042	+33 (0)3 89 76 01 24	+31 (0)548 659044

Appendix B:

ABRASIVES

Cemented Carbide Grade

K40L

PHYSICAL AND METALLURGICAL PROPERTIES				
Composition	12.0% Co ± 0.2		0.15% VC	87.85% WC
Density	14.30	±	0.10	g/cm³
Magnetic Saturation	207 16.5	- -	239 19.0	0.1μTm³/kg Gcm³/g
Coercivity*	10.3 130	- -	12.7 160	kA/m Oe
Hardness	1270 89.0	± ±	50 0.3	HV20 HRA
TRS (ISO 3327)	3400			N/mm² MPa
Compressive Strength	4000			N/mm² MPa
Young's Modulus (E-Modulus)	610	±	10	kN/mm² GPa
Poisson's Ratio	0.22	±	0.01	
Thermal Expansion	6.5	±	0.3	10^{-6}/K

** Guideline.*

SINTERED WC GRAIN SIZE	PRIME USES
Medium	Medium wear, medium impact

TYPICAL MICROSTRUCTURE

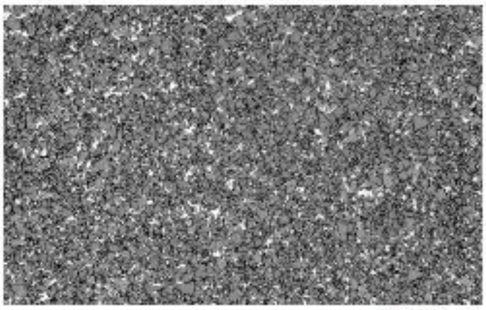

10μm

CORROSION

MASS LOSS (mg/cm²/day)

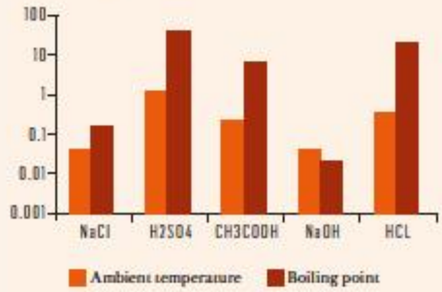

Element Six is constantly striving to improve its products and therefore reserves the right to change materials and specifications without prior notice.

This product has been manufactured under the controls established by a Bureau Veritas Certification approved management system.

EMAS

FOR MORE INFORMATION

Contact an Element Six representative:
Call: +49 (0) 6652 820
Email: hm@e6.com
Website: www.e6.com

elementsix.
a De Beers Group Company

62.01

Appendix C:

ALPHAFORM LF

Low to Medium Frequency Soft Magnetic Composite [Frequency Range: 1 – 80 kHz]

Formable soft magnetic composite developed on the basis of magnetic particles with a thermal-curing epoxy binder. This material may be used for quick and efficient installation to induction coils with low tolerances. No additional electrical insulation of the coil turns is necessary.

Properties	Units	ALPHAFORM LF
Density ± 2%	g/cm3	4.1
Initial Permeability	None	11
Maximum Permeability	None	13
Saturation Flux Density	T	1.0
Operating Frequency Range	kHz	1–80
Major Frequency Range	kHz	3–50
Temperature Resistance	Centigrade	225 Long Term 300 Short Term
Thermal Conductivity	W/cm °C	0.02
Resistivity	kOhmcm	>15

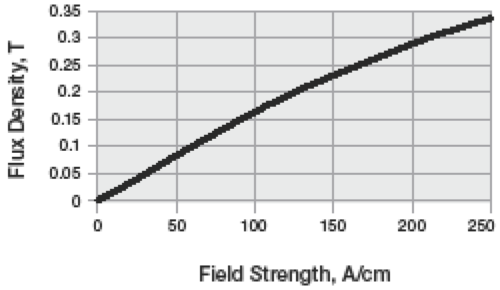

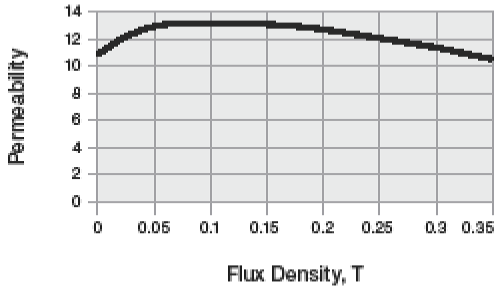

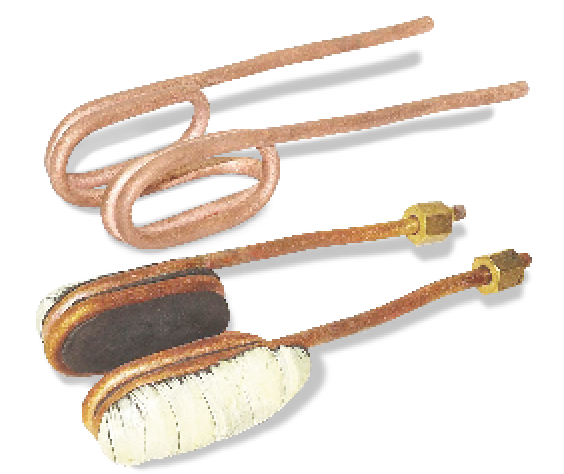

AlphaForm LF core dramatically increased efficiency of the "earmuff" brazing coil

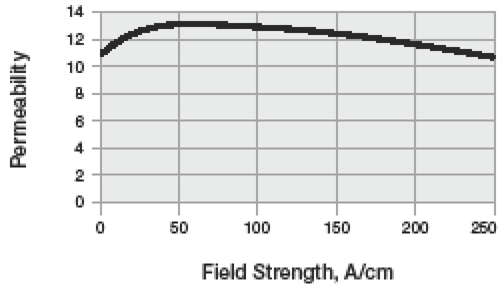

Each grade of Fluxtrol material has its own distinctive properties that are the most beneficial to certain application conditions, process type, coil design, frequency, etc. Contact Fluxtrol or your local distributor for more information about which material is optimal for you.

FLUXTROL 100 | FLUXTROL A | FLUXTROL 50 | FERROTRON 559H | ALPHAFORM LF

FLUXTROL
1388 Atlantic Blvd. | Auburn Hills, MI 48326 USA | P: 1.248.393.2000 | 1.800.224.5522 USA | F: 1.248.393.0277 | fluxtrol.com